Quantum Chemical Molecular Dynamics Simulations of SWNT Nucleation and Growth on Iron and Nickel

Stephan Irle
Institute for Advanced Research and Department of Chemistry
Nagoya University, Nagoya Japan

GCOE for Mechanical Systems Innovation (GMSI) Seminar
The University of Tokyo, Tokyo, December 2, 2009

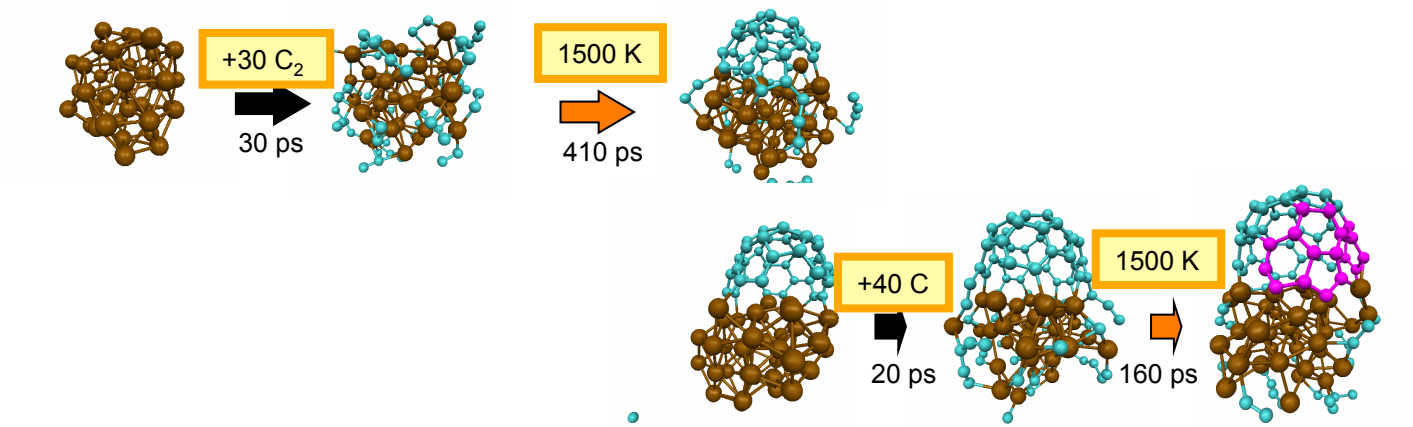

Acknowledgement to Collaborators

Japan Science and Technology Agency

Prof. Keiji Morokuma

Students and PD fellows:

Dr. Guishan Zheng[a]

Dr. Yoshiko Okamoto

Dr. Zhi Wang

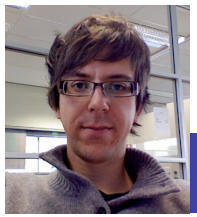

Dr. Alister J. Page

Dr. Yasuhito Ohta[b]

Dr. Ying Wang

[a]now: Department of Chemistry, Harvard University

[b]now: Professor, Nara Women's University

Outline

- Review: Experiments and previous theoretical modeling
- Density-functional tight-binding (DFTB) method
- All-carbon cap nucleation and growth on iron particles
- Comparison of growth mechanisms between iron and nickel catalysts
- Simulation of early stages during ACCVD (C_2H_2 and OH on iron catalyst)
- Summary and outlook

Outline

- **Review: Experiments and previous theoretical modeling**
- **Density-functional tight-binding (DFTB) method**
- **All-carbon cap nucleation and growth on iron particles**
- **Comparison of growth mechanisms between iron and nickel catalysts**
- **Simulation of early stages during ACCVD (C_2H_2 and OH on iron catalyst)**
- **Summary and outlook**

Irreversible Steps of Giant Fullerene Formation

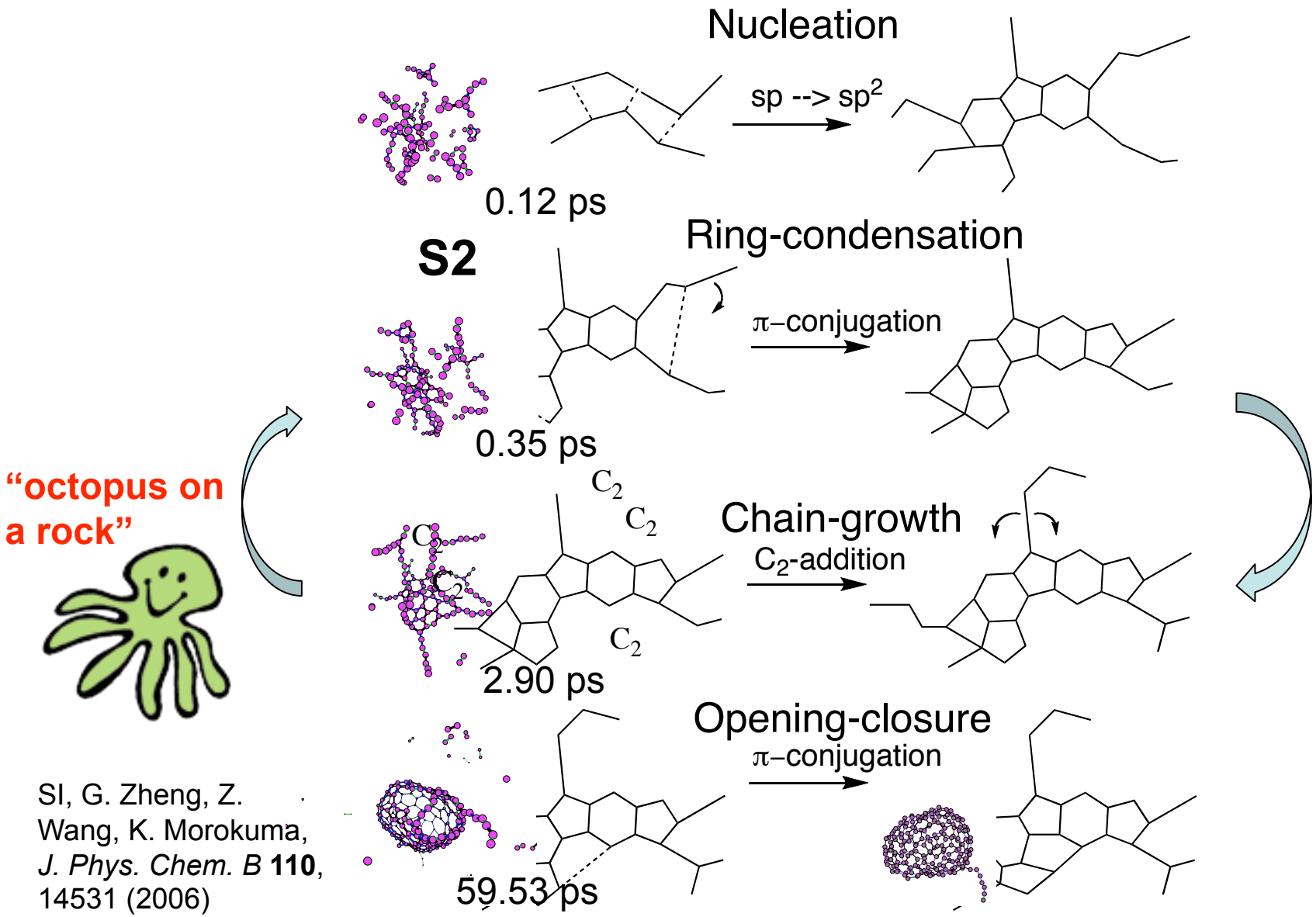

SI, G. Zheng, Z. Wang, K. Morokuma, *J. Phys. Chem. B* **110**, 14531 (2006)

Experimental sizes of fullerene cages …

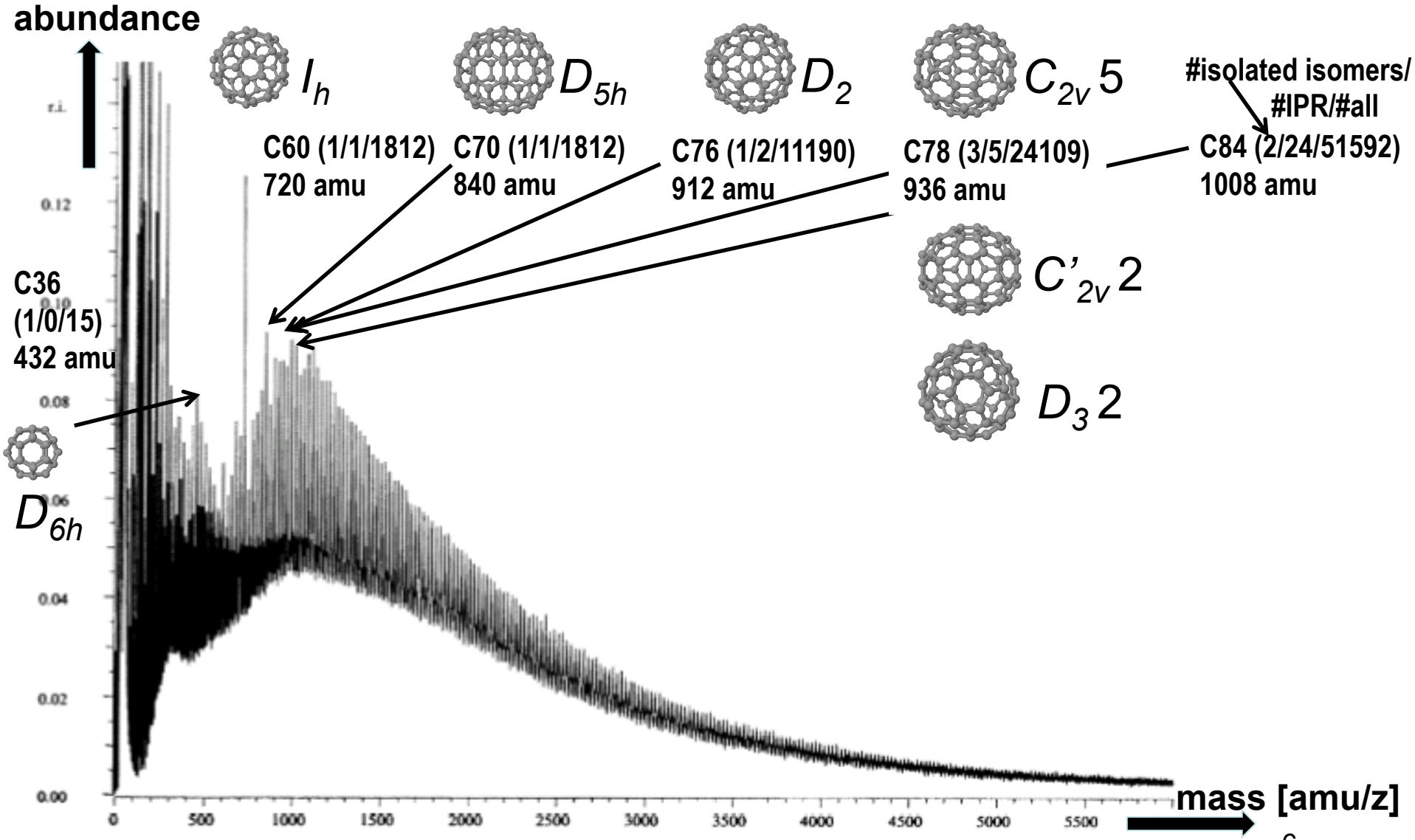

Source: Johnson *et al.*, Carbon **40**, 189 (2002)

… explained by Shrinking Hot Giant Road

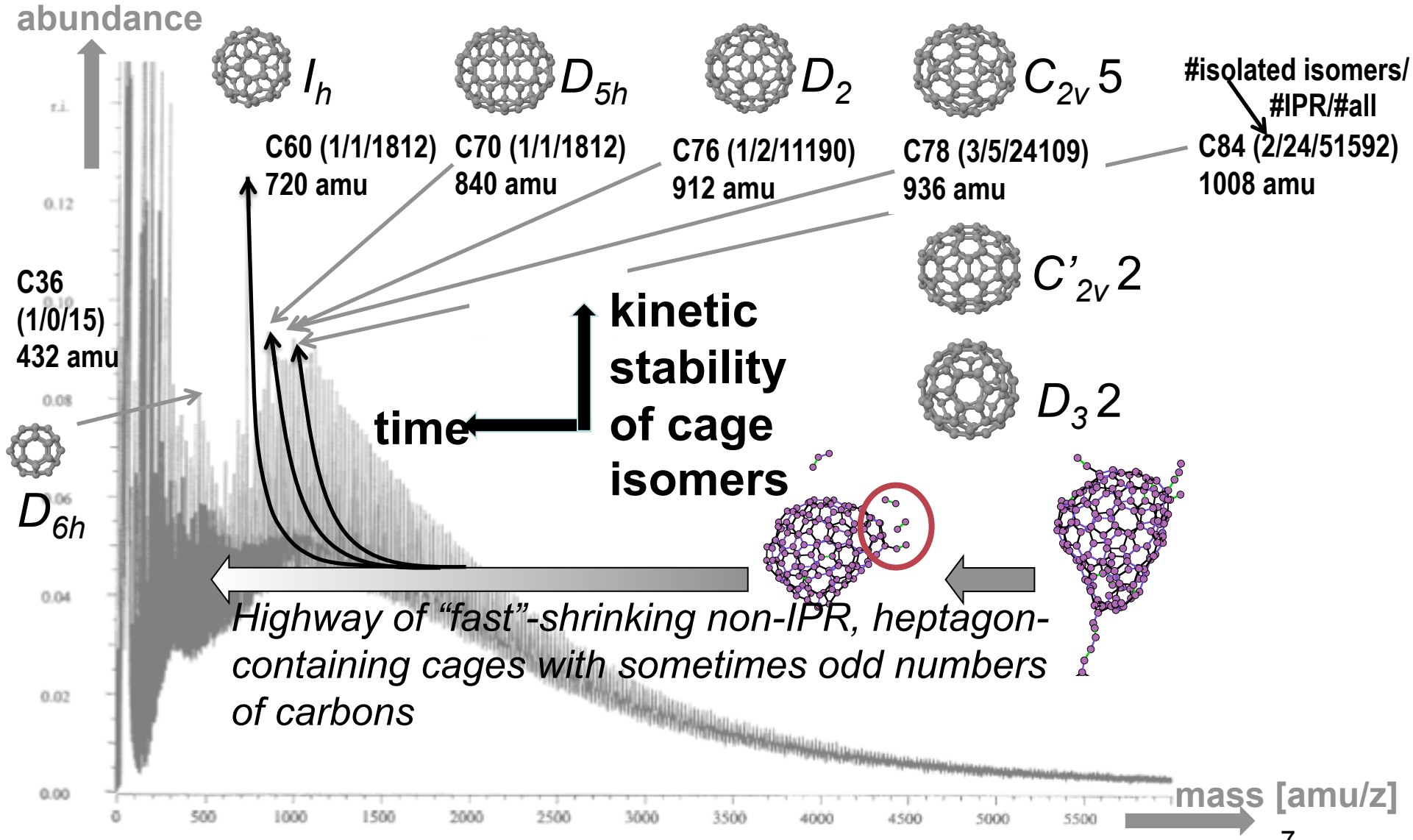

Source: Johnson *et al.*, Carbon **40**, 189 (2002)

"Unusual" Case: CNT Growth from *C-face* SiC Surface During High-Temp. Vacuum Evaporation

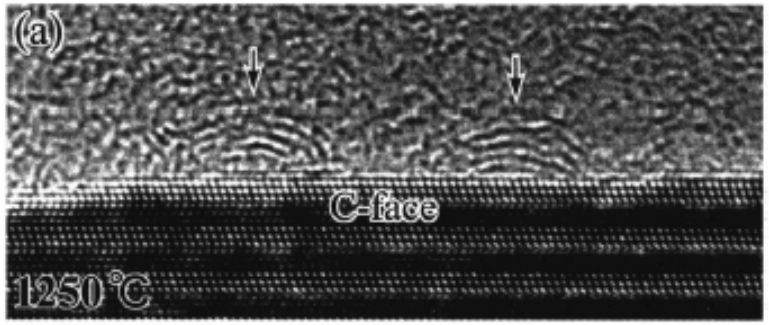

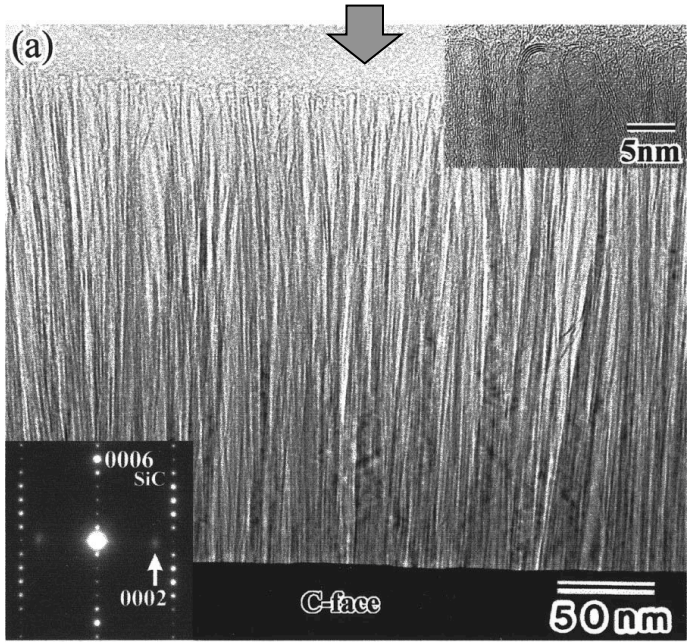

M. Kusunoki, *et al. Appl. Phys. Lett.* **77**, 531 (2000)

Zhi Wang, SI, G. Zheng, M. Kusunoki, K. Morokuma, *J. Phys. Chem. C* **111**, 12960 (2007)

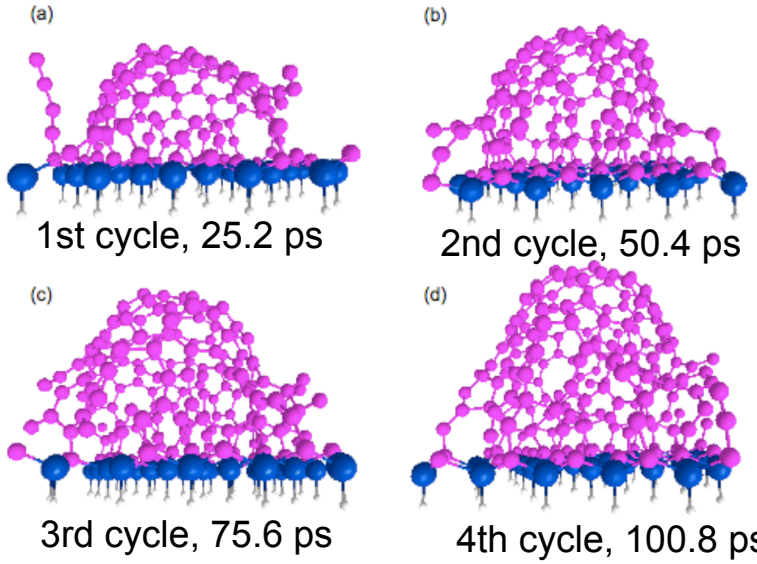

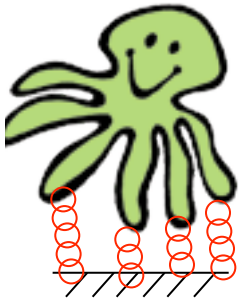

Δt(Si removal) = 0.24 ps
T = 2000 K

But: Graphene Growth from *Si-face* SiC Surface During High-Temp. Vacuum Evaporation

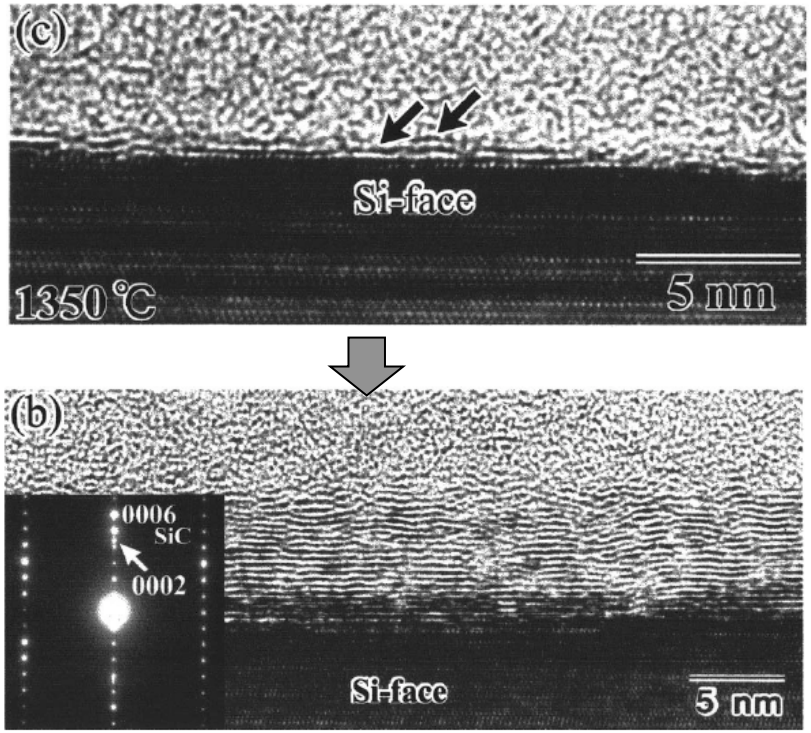

Zhi Wang, SI, G. Zheng, M. Kusunoki, K. Morokuma, *J. Phys. Chem. C* **111**, 12960 (2007)

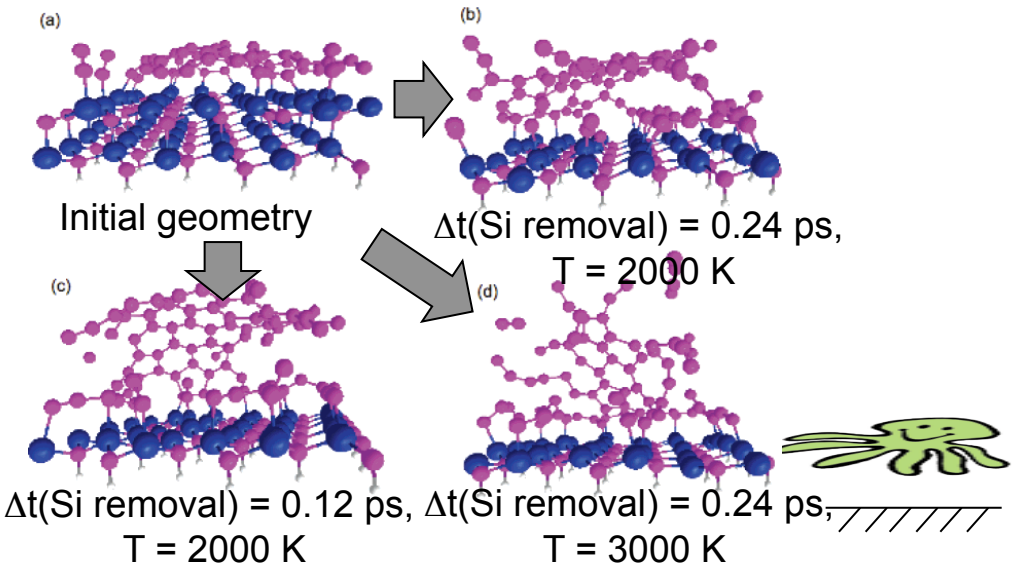

Adhesion energies:

Graphene-C > Graphene-Si
(dome) (sheet)

M. Kusunoki, *et al. Appl. Phys. Lett.* **77**, 531 (2000)

A Nobelist's Perspective

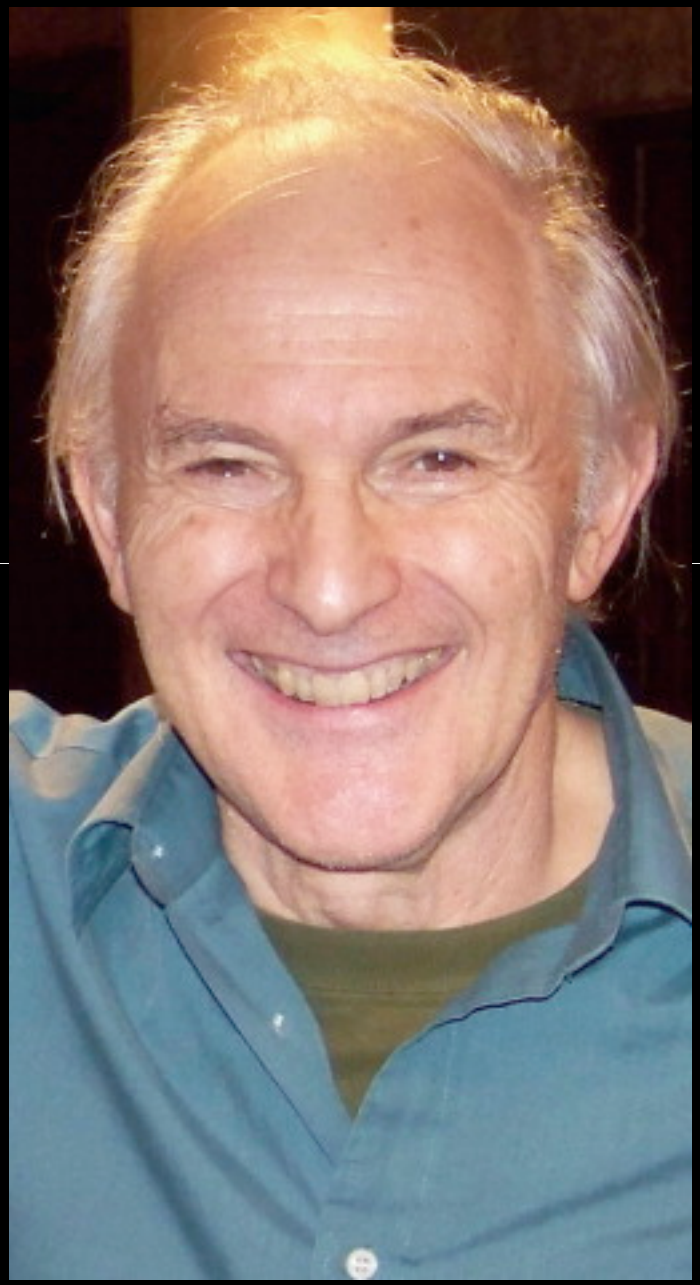

"They [nanotubes and nanowires] have to have reproducible properties, and we're not in that situation at the present time; you can make various types of nanotubes and study the properties of them but at the moment we don't have the control to produce the nanotubes with accurately specified diameter, structure, chirality, you name it."

Sir Harry Kroto in D. J. Palmer, Where nano is going, *Nano Today* **3**, 46 (2008)

Recent advancements in SWNT growth control

◆Diameter control:

➢C. Lu and J. Liu, Controlling the Diameter of Carbon Nanotubes in Chemical Vapor Deposition Method by Carbon Feeding, *J. Phys. Chem. B* **110**, 20254 (2006)

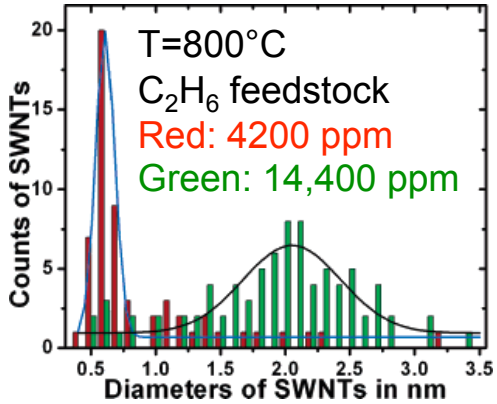

➢H. Shinohara and coworkers: Synthesis of single-wall carbon nanotubes grown from size-controlled Rh/Pd nanoparticles by catalyst-supported chemical vapor deposition, *Chem. Phys. Lett.* **458**, 346 (2008)

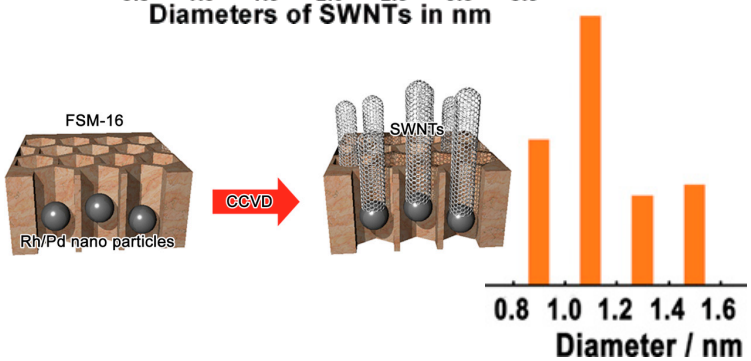

◆Chirality control:

➢D. E. Resasco, R. B. Weisman, and coworkers, Narrow (n,m)-Distribution of Single-Walled Carbon Nanotubes Grown Using a Solid Support Catalyst, *J. Am. Chem. Soc.* **125**, 11186 (2003)

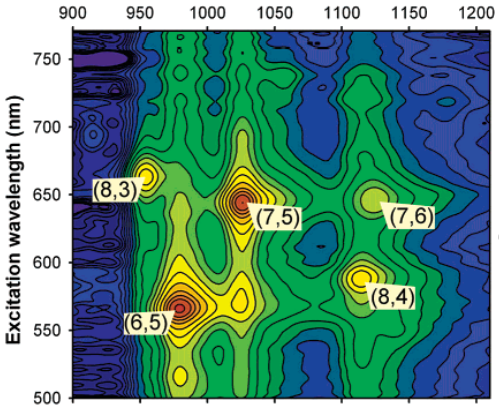

CoMoCAT: Co-Mo catalyst

Many others ...

Other improvements

◆High yield:

➢K. Hata, D. Futaba, *et al.* Water-Assisted Highly Efficient Synthesis of Impurity-Free Single-Walled Carbon Nanotubes, *Science* **306**, 1362 (2004)

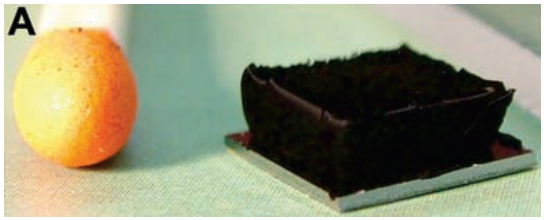

so-called "supergrowth"

◆Defect control:

➢S. Maruyama *et al.*, Low-temperature synthesis of high-purity single-walled carbon nanotubes from alcohol, *Chem. Phys. Lett.* **360**, 229 (2002)

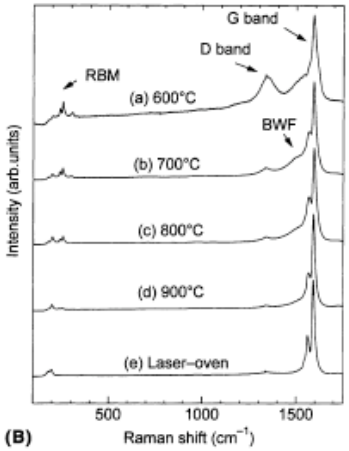

Low Raman D/G ratio = high purity when using alcohols as feedstock (ACCVD)

◆Length control:

➢L. X. Zheng *et al.*, Ultralong single-wall carbon nanotubes, *Nature Mater.* **3**, 673 (2004)

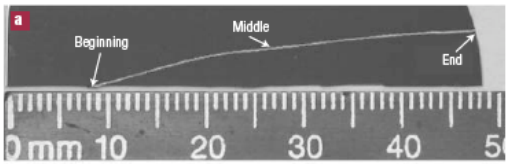

Many other groups and improvements …

But … How to put the puzzle pieces together?

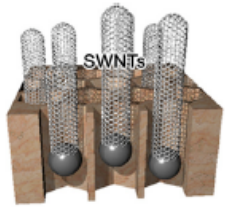

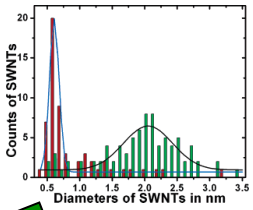

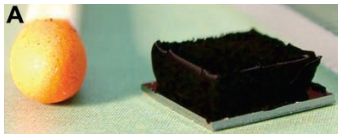

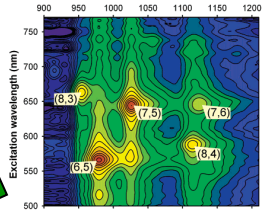

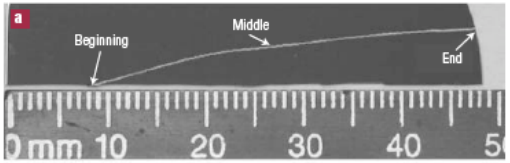

ACCVD etc …

Selection of "appropriate" growth conditions

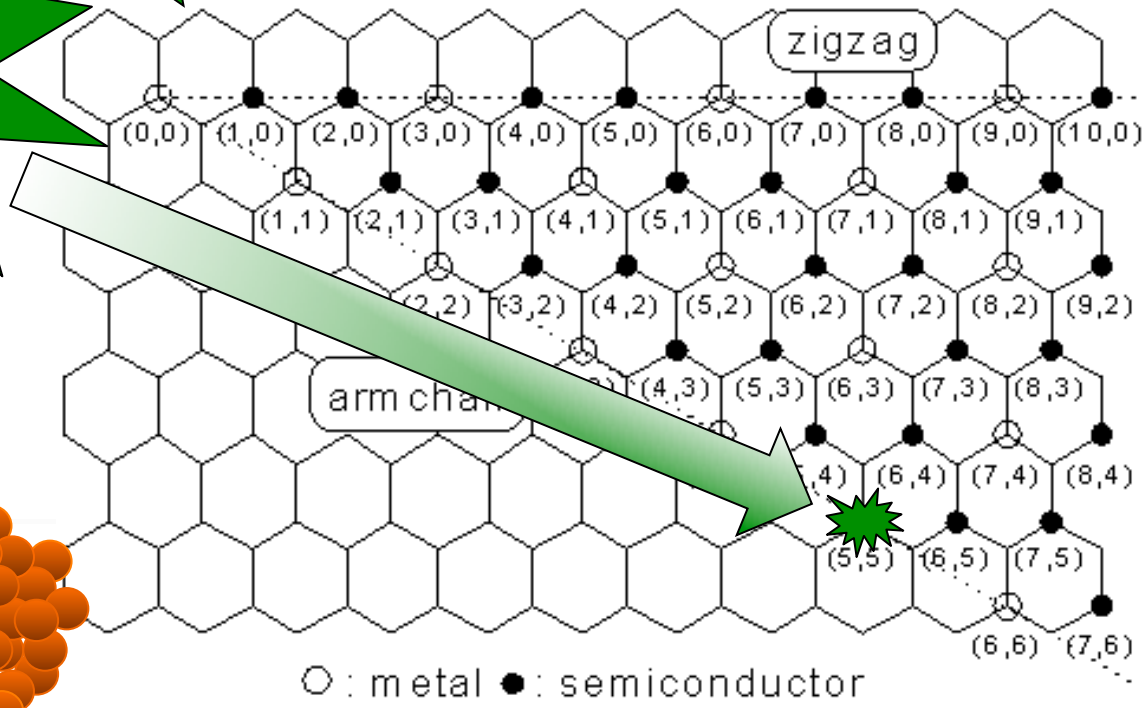

(5,5) SWNT

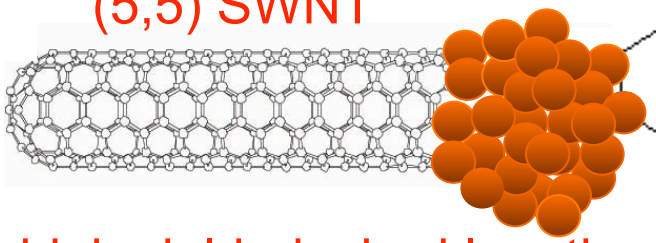

high yield, desired length, defect-free, eventually catalyst-free

Look here … *in situ* environmental TEM studies of SWNT nucleation and growth

F. Ding, *et al.* *Appl. Phys. Lett.* **88**, 133110 (2006)

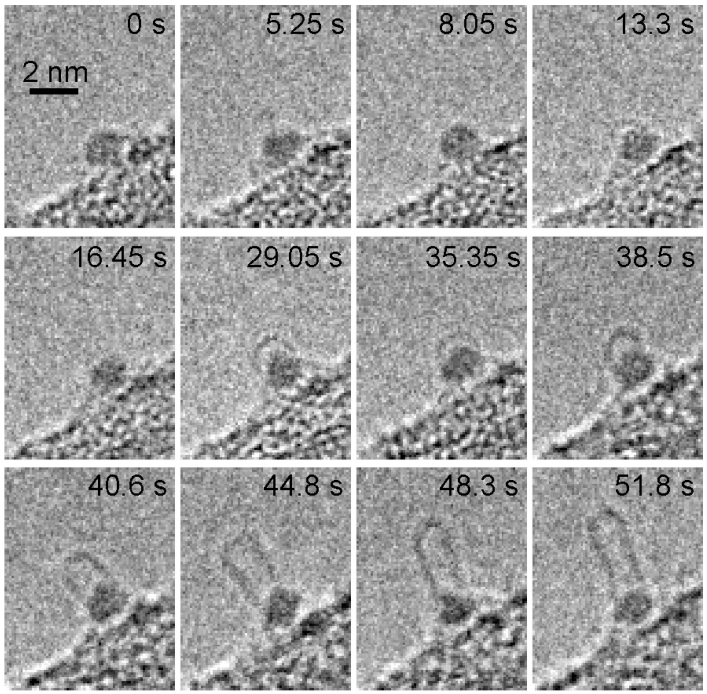

Fe/SiO_2 $C_2H_2:H_2$ T=600°C

Fluctuating solid **Fe_3C**

H. Yoshida, *et al.* Atomic-Scale In-situ Observation of Carbon Nanotube Growth from Solid State Carbide Nanoparticles, *Nano Lett.* **8**, 2082 (2008)

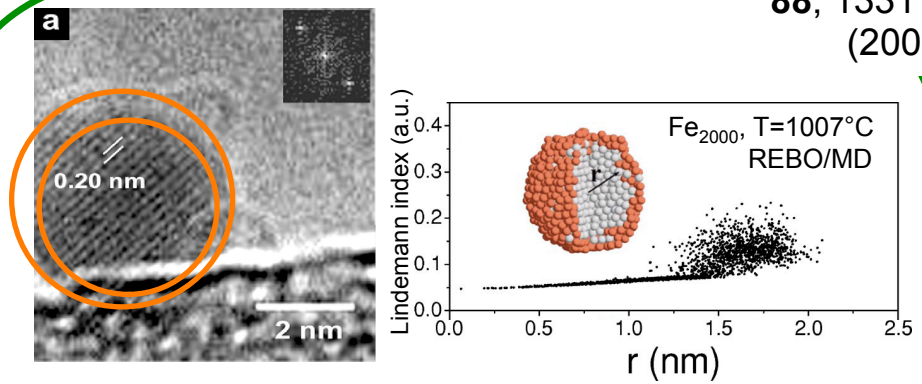

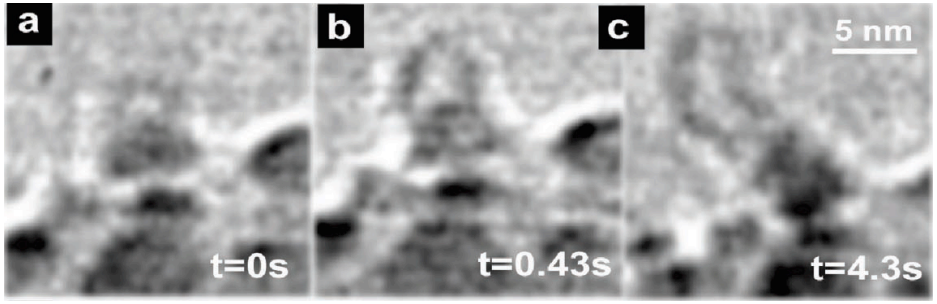

Ni/SiO_2 $C_2H_2:NH_3$ T=480 to 700°C

Fluctuating solid **pure nickel**

S. Hofmann, *et al.* In-situ Observations of Catalyst Dynamics during Surface-Bound Carbon Nanotube Nucleation, *Nano Lett.* **7**, 602 (2007)

SWNT Growth N-dimensional "Parameter Space"

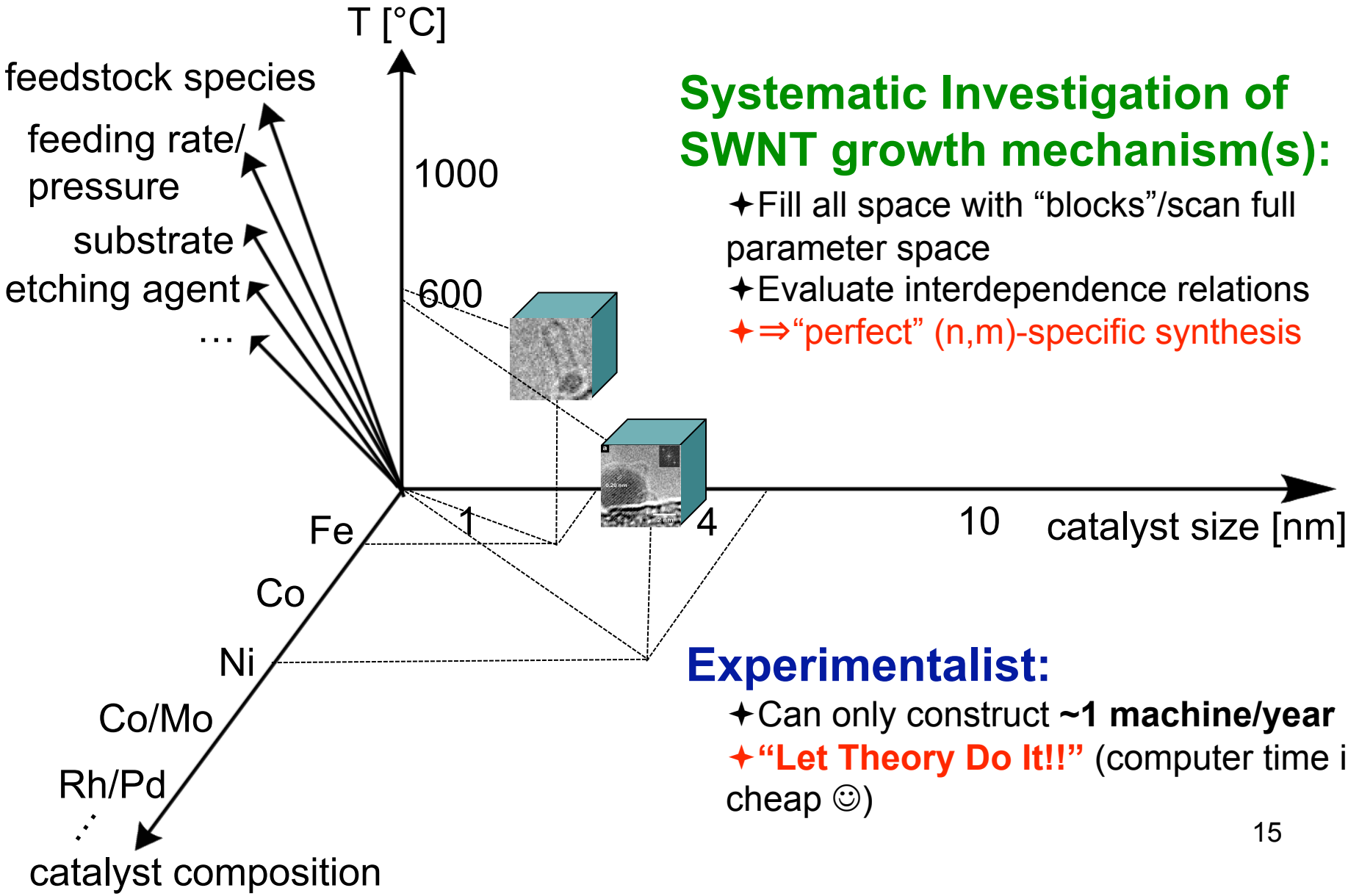

Systematic Investigation of SWNT growth mechanism(s):

- ✦Fill all space with "blocks"/scan full parameter space
- ✦Evaluate interdependence relations
- ✦⇒"perfect" (n,m)-specific synthesis

Experimentalist:

- ✦Can only construct **~1 machine/year**
- ✦**"Let Theory Do It!!"** (computer time is cheap ☺)

Previous Car-Parrinello Molecular Dynamics (CPMD)

Heroic efforts on supercomputers, one-shot simulations!

J. Gavillet *et al,* Root-Growth Mechanism for SWNTs, *Phys. Rev, Lett.* **87**, 275504 (2001)

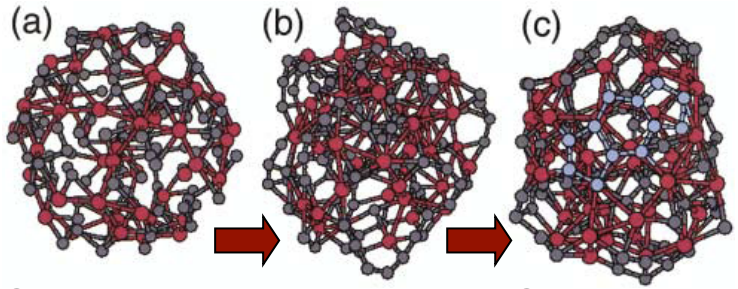

Carbon precipitation on Co carbide particle, 51 Co & 102 C atoms, 25 ps ⇒ 1 hexagon, 2 pentagons

C_{30}+44C on Co surface at 1500 K, 15 ps ⇒ 5 carbon atoms diffused to cap

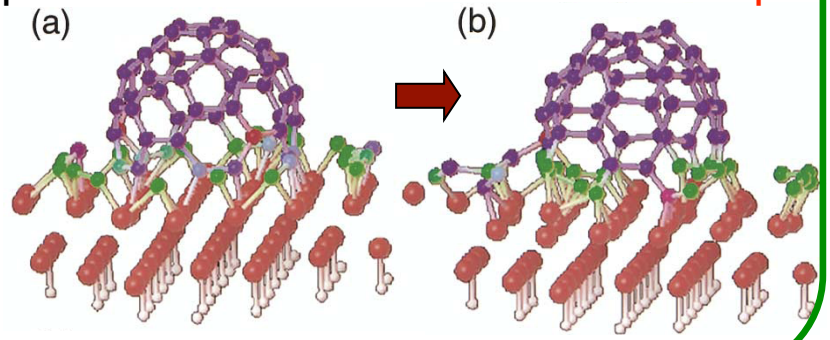

J.-Y. Raty *et al,* Growth of Carbon Nanotubes on Metal Nanoparticles: A Microscopic Mechanism from *Ab Initio* Molecular Dynamics Simulations, *Phys. Rev, Lett.* **95**, 096103 (2005)

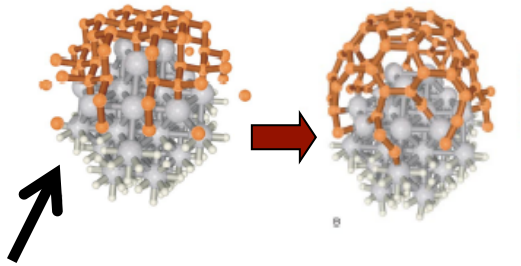

Change from diamond structure (sp^3) to fullerene cap (sp^2) immediately!

Nano-diamond: Inappropriate model!

simulation time~10 ps
Too short to demonstrate self-assembly

Reactive Empirical Bond Order (REBO) MD

Classical potential, cheap, allows many long simulations!

Bond order potential allows bond breaking via potential switching functions, but does not include effects of π-conjugation or charge transfer

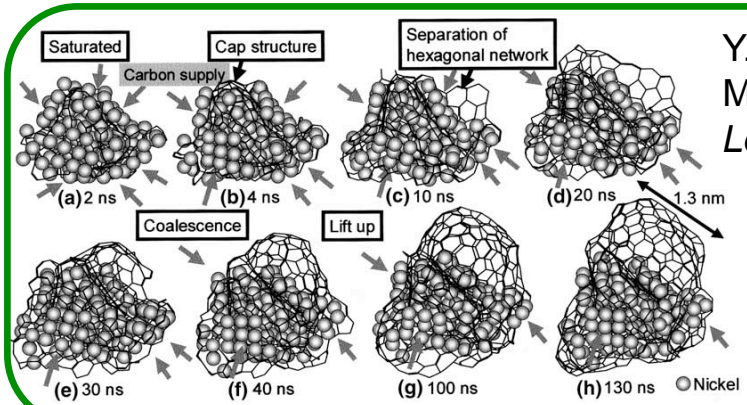

Y. Shibuta & S. Maruyama, *Chem. Phys. Lett.* **382**, 381 (2003)

500 C atoms +nC, Ni_{108}, T=2227°C (20 nm)^3 PBC

Y. Shibuta & S. Maruyama, *Chem. Phys. Lett.* **437**, 218 (2003)

500 C atoms +nC, Ni_{256} on LJ support T=2227°C (20 nm)^3 PBC

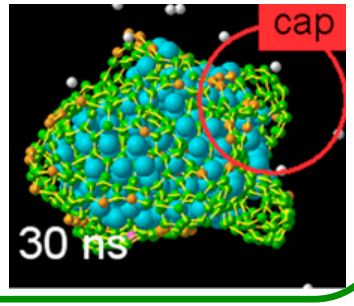

F. Ding *et al.*, *J. Phys. Chem. B* **108**, 17369 (2004)

Feeding carbon atoms from center of Fe clusters: Fe50 + nC, T=627°C

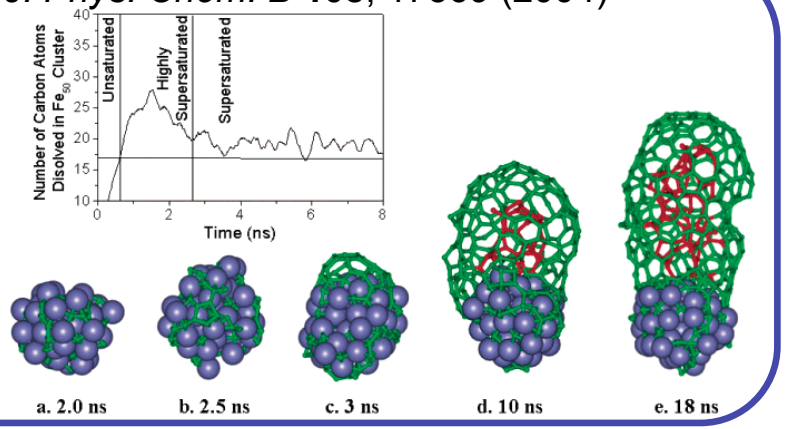

F. Ding *et al.*, *J. Chem. Phys.* **121**, 2775 (2004)

Fe_m + nC, T=527°C to 627°C

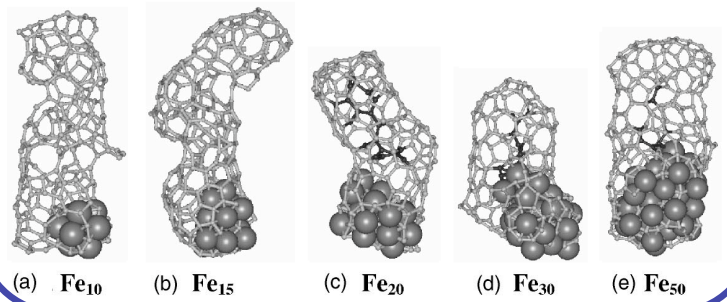

Many more studies …

Specific problems of REBO MD for SWNT growth

•Problem 1: large number of non-hexagon rings!

REBO does not discriminate between aromatic or antiaromatic rings
➔*Unrealistically many 4- and 8-membered rings (formally antiaromatic)*

F. Ding *et al.*, *J. Phys. Chem. B*, **108**, 17369 (2004)

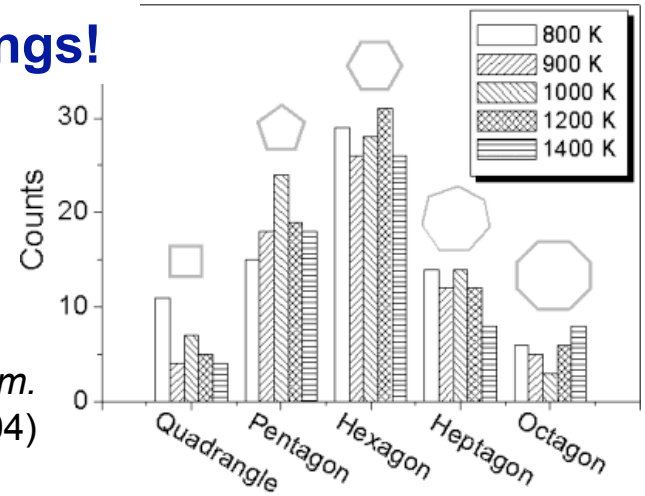

•Problem 2: polyynes are underrepresented

Important for self-healing of graphitic sheets
⇒*Very slow transformation processes*
G. Zheng, SI, M. Elstner, K. Morokuma, *J. Phys. Chem. A* **108**, 3182 (2004)

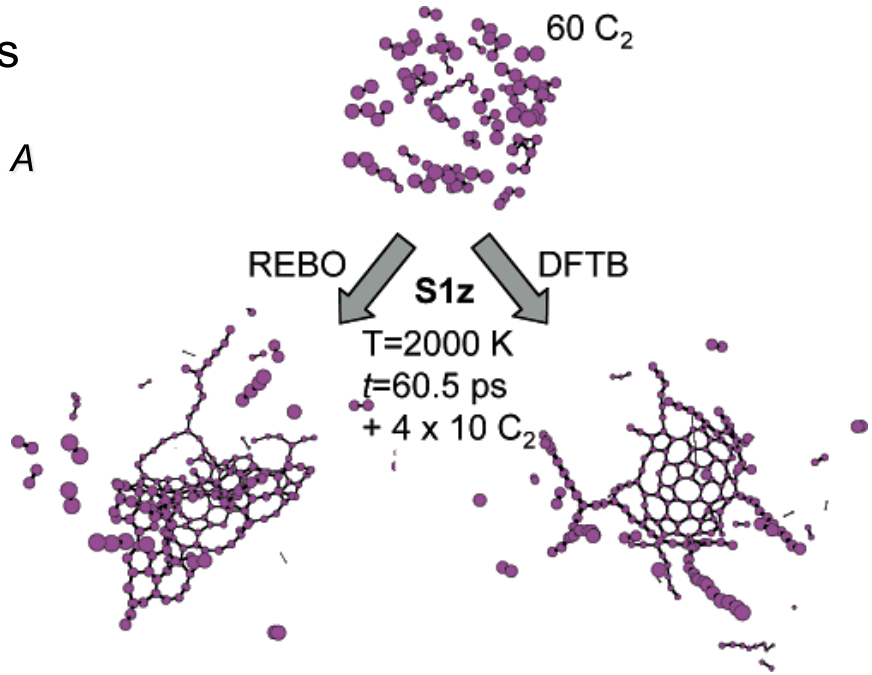

•Problem 3: sp^3 defects overestimated

➔*Amorphous structure formation*

•N. A. Marks *et al.*, *Phys. Rev. B* **65**, 075411 (2002)
•SI, G. Zheng, Z. Wang, K. Morokuma, *J. Phys. Chem. B* **110**, 14531 (2006)

Outline

- Review: Experiments and previous theoretical modeling
- **Density-functional tight-binding (DFTB) method**
- All-carbon cap nucleation and growth on iron particles
- Comparison of growth mechanisms between iron and nickel catalysts
- Simulation of early stages during ACCVD (C_2H_2 and OH on iron catalyst)
- Summary and outlook

Density-Functional Tight-Binding (DFTB)

Extended Hückel type method using atomic parameters from DFT (PBE, GGA-type), diatomic repulsive potentials from B3LYP

- Seifert, Eschrig (1980-86): STO-LCAO; 2-center approximation
- Porezag, Frauenheim, *et al.* (1995): efficient parameterization scheme: ***NCC-DFTB***

Gotthard Seifert

Thomas Frauenheim

- Elstner *et al.* (1998): charge self-consistency: ***SCC-DFTB***
- Köhler *et al.* (2001): spin-polarized DFTB: ***SDFTB***

$$E^{(NCC-)DFTB} = \sum_{i}^{\substack{valence\\orbitals}} n_i \varepsilon_i + \frac{1}{2} \sum_{A \neq B}^{atoms} E_{AB}^{rep}$$

$$E^{(SCC-)DFTB} = E^{(NCC-)DFTB} + \frac{1}{2} \sum_{A \neq B}^{atoms} \gamma_{AB} \Delta q_A \Delta q_B$$

$$E^{S(pin-polarized)DFTB} = E^{(SCC-)DFTB} + \frac{1}{2} \sum_{A}^{atoms} \sum_{l \in A} \sum_{l' \in A} p_{Al} p_{Al'} W_{All'}$$

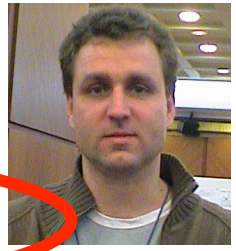

Marcus Elstner

Christof Köhler

Self-Consistent-Charge Density-Functional Tight-Binding (SCC-DFTB)

M. Elstner *et al.*, *Phys. Rev. B* **58** 7260 (1998)

Approximate density functional theory (DFT) method!

Second-order Taylor expansion of variational DFT energy in terms of atomic reference density ρ_0 and charge fluctuation ρ_1 ($\rho \cong \rho_0 + \rho_1$) yields:

$$E[\rho] = \underbrace{\sum_{i}^{\substack{\text{valence}\\\text{orbitals}}} n_i \langle \phi_i | \hat{H}[\rho_0] | \phi_i \rangle}_{1} + \underbrace{\sum_{i}^{\substack{\text{core}\\\text{orbitals}}} n_i \langle \phi_i | \hat{H}[\rho_0] | \phi_i \rangle}_{2} + \underbrace{E_{\text{xc}}[\rho_0]}_{3} - \underbrace{\frac{1}{2}\int_{\mathbf{R}^3} \rho_0 V_H[\rho_0]}_{4} -$$

$$- \underbrace{\int_{\mathbf{R}^3} \rho_0 V_{\text{xc}}[\rho_0]}_{5} + \underbrace{E_{\text{nucl}}}_{6} + \underbrace{\frac{1}{2}\int_{\mathbf{R}^3} \rho_1 V_H[\rho_1]}_{7} + \underbrace{\frac{1}{2}\iint_{\mathbf{R}^3} \left.\frac{\delta^2 E_{\text{xc}}}{\delta \rho_1^2}\right|_{\rho_0} \rho_1^2}_{8} + o(3)$$

Density-functional tight-binding (DFTB) method is derived from terms 1-6 (zero-order terms)

Self-consistent-charge density-functional tight-binding (SCC-DFTB) method is derived from terms 1-8 (zero- & second-order terms)

DFTB and SCC-DFTB methods

$$E^{\mathrm{DFTB}} = \underbrace{\sum_{i}^{\substack{\text{valence}\\\text{orbitals}}} n_i \varepsilon_i}_{\text{term 1}} + \underbrace{\frac{1}{2}\sum_{A\neq B}^{\text{atoms}} E_{\mathrm{rep}}^{AB}}_{\text{terms 2–6}}$$

$$E^{\mathrm{SCC-DFTB}} = \underbrace{\sum_{i}^{\substack{\text{valence}\\\text{orbitals}}} n_i \varepsilon_i}_{\text{term 1}} + \underbrace{\frac{1}{2}\sum_{A\neq B}^{\text{atoms}} \gamma_{AB}\Delta q_A \Delta q_B}_{\text{terms 7–8}} + \underbrace{\frac{1}{2}\sum_{A\neq B}^{\text{atoms}} E_{\mathrm{rep}}^{AB}}_{\text{terms 2–6}}$$

- where
  - n_i and ε_i — occupation and orbital energy ot the ith Kohn-Sham eigenstate
  - E_{rep} — distance-dependent diatomic repulsive potentials
  - Δq_A — induced charge on atom A
  - γ_{AB} — distance-dependent charge-charge interaction functional; obtained from atomic chemical hardness $\eta_{AA} = 1/2(\mathrm{IP_A} - \mathrm{EA_A})$

SCC-DFTB: general comparison with experiment

Performance for small organic molecules
(mean absolut deviations)

- Reaction energies: ~ 5 kcal/mol
- Bond lenghts: ~ 0.014 A°
- Bond angles: ~ 2°
- Vibrational frequencies: ~6-7 %

Self-consistent-charge density-functional tight-binding (SCC-DFTB)

D. Porezag, Th. Frauenheim, T. Köhler, G. Seifert, R. Kaschner, *Phys. Rev. B* **51,** 12947 (1995)
M. Elstner *et al., Phys. Rev. B* **58,** 7260 (1998)

Second order-expansion of DFT total energy with respect to charge fluctuation

TB-eigenvalue equation $\sum_{\nu} c_{\nu i}\left(H_{\mu\nu} - \varepsilon_i S_{\mu\nu}\right) = 0$ Single-zeta STO basis set

$$E_{tot} = 2\sum_i f_i \varepsilon_i + E_{rep} + \frac{1}{2}\sum_{\alpha\beta} \gamma_{\alpha\beta} \Delta q_\alpha \Delta q_\beta$$

Finite temperature approach (Mermin free energy E_{Mermin})

M. Weinert, J. W. Davenport, *Phys. Rev. B* **45**, 13709 (1992)

$$f_i = \frac{1}{\exp\left[\left(\varepsilon_i - \mu\right)/k_B T_e\right] + 1}$$

T_e: electronic temperature
S_e: electronic entropy

$$0 \le f_i \le 1$$

$$E_{Mermin} = E_{tot} - T_e S_e$$

$$S_e = -2k_B \sum_i^{\infty} f_i \ln f_i + \left(1 - f_i\right)\ln\left(1 - f_i\right)$$

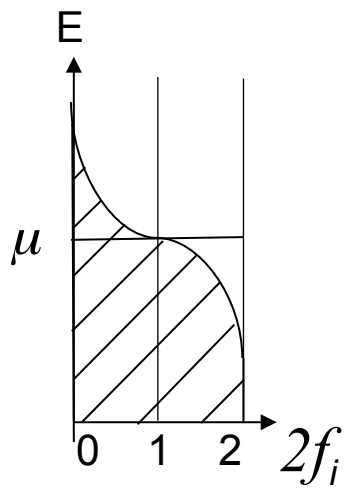

Atomic force

$$\vec{F}_\alpha = -2\sum_i f_i \sum_{\mu\nu} c_{\mu i} c_{\nu i}\left[\frac{\partial H^0_{\mu\nu}}{\partial \vec{R}_\alpha} - \left(\varepsilon_i - \frac{H^1_{\mu\nu}}{S_{\mu\nu}}\right)\frac{\partial S_{\mu\nu}}{\partial \vec{R}_\alpha}\right] - \Delta q_\alpha \sum_\xi^N \frac{\partial \gamma_{\alpha\xi}}{\partial \vec{R}_\alpha}\Delta q_\xi - \frac{\partial E_{rep}}{\partial \vec{R}_\alpha}$$

(5,5) armchair SWNT ($H_{10}C_{60}$) + Fe / Fe_{55}

Y. Ohta, Y. Okamoto, SI, K. Morokuma, Phys. Rev. B **79**, 195415 (2009)

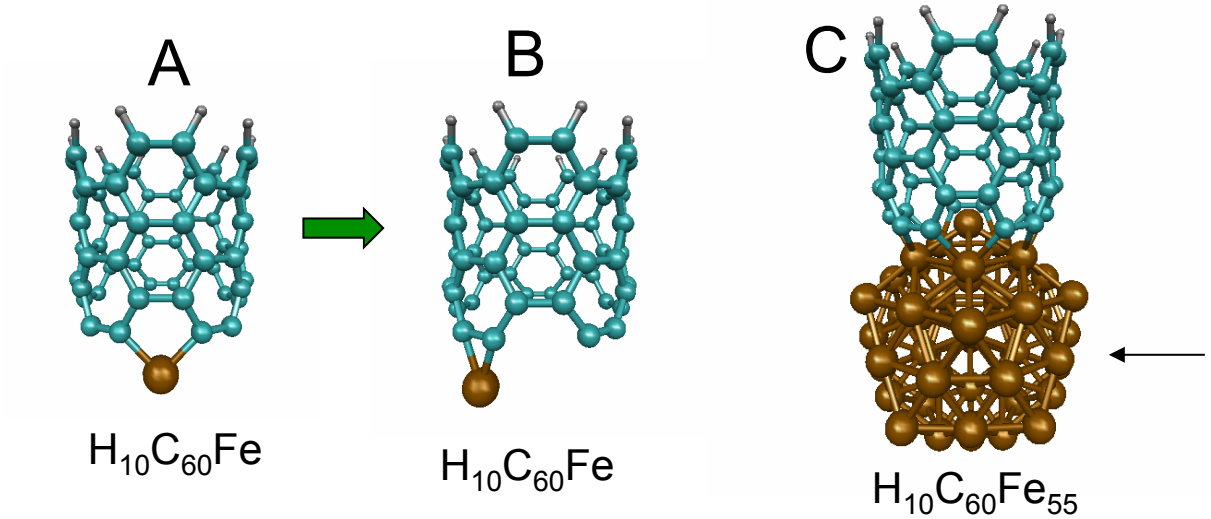

Fe_{55} icosahedron,

P. Larsson *et al.* Phys. Rev. B **75**, 115419 (2007)

Adhesion energies (eV/atom)

	A	B	C
DFT:PW91[1]	-6.24	-5.63	-1.82
SCC-DFTB[2]	-5.17	-4.68	-1.86

[1] Phys. Rev. B **75**, 115419 (2007) [2] Fermi broadening=0.13 eV

[1]: PW91: An ultrasoft pseudopotential with a plane-wave cutoff of 290 eV for the single metal and the projector augmented wave method with a plane-wave cutoff of 400 eV for the metal cluster

{2} Fe-Fe and Fe-C DFTB parameters from: G. Zheng *et al., J. Chem. Theor. Comput*. **3**, 1349 (2007)

Outline

- Review: Experiments and previous theoretical modeling
- Density-functional tight-binding (DFTB) method
- **All-carbon cap nucleation and growth on iron particles**
- Comparison of growth mechanisms between iron and nickel catalysts
- Simulation of early stages during ACCVD (C_2H_2 and OH on iron catalyst)
- Summary and outlook

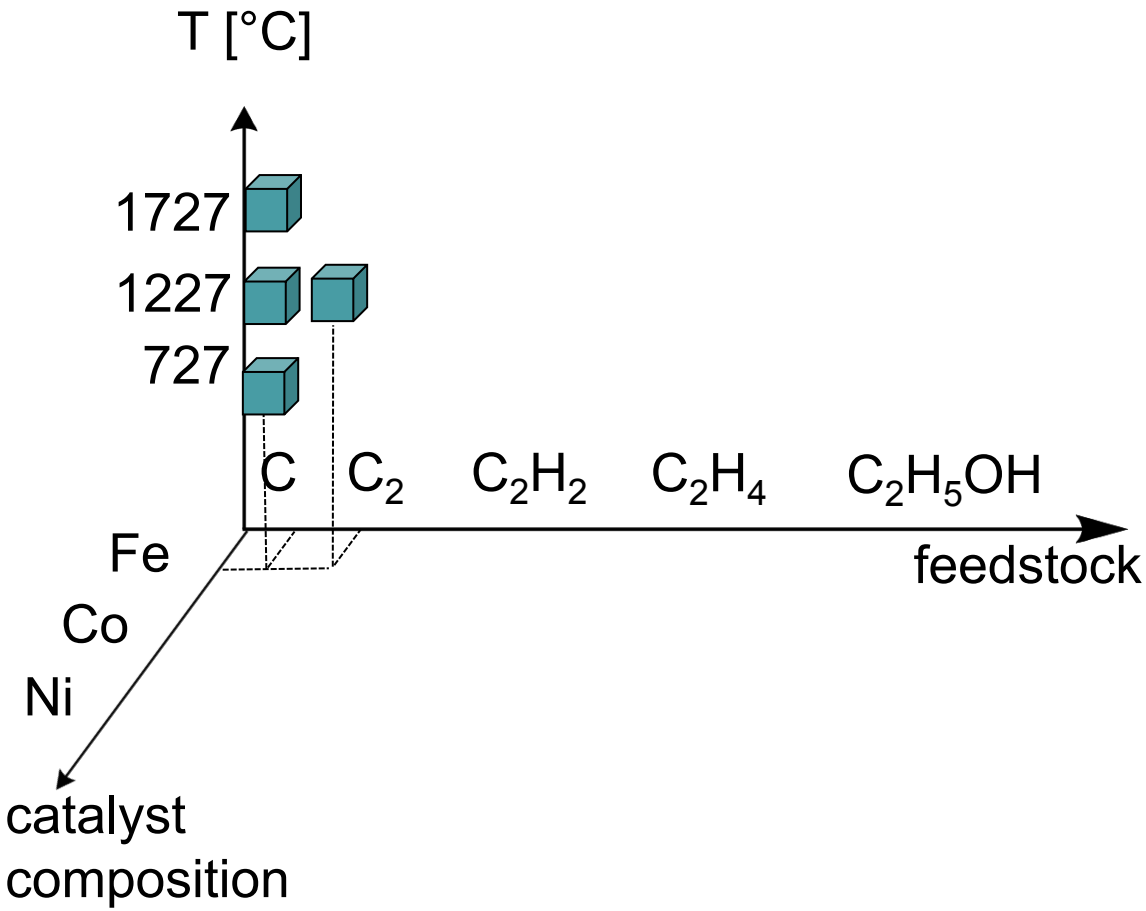

Dr. Yasuhito Ohta[b]

[b]now: Professor, Nara Women's University

Dr. Yoshiko Okamoto

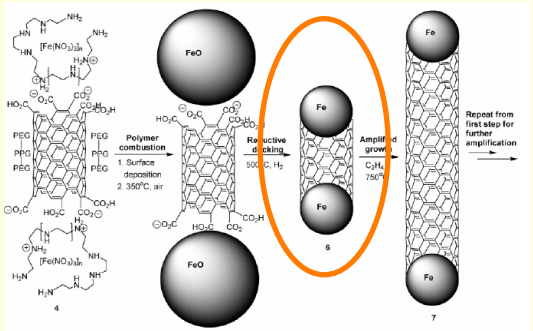

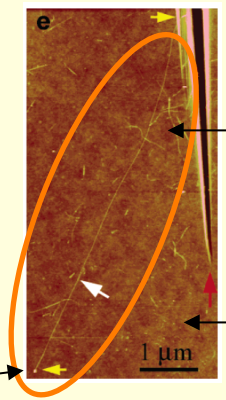

Diameter: ~1nm

Silicon-oxide

Fe particle

R.E. Smalley et al. JACS 128, 15824 (2006)

Model system and carbon supply

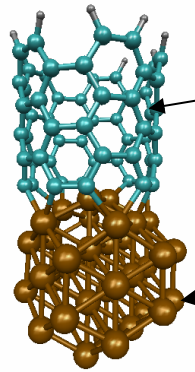

(5,5) armchair SWNT

length = 6.2 Å
diameter = 7.5 Å

fcc Fe_{38}

Total: 108 atoms

Y. Ohta, Y. Okamoto, SI, K. Morokuma, *ACS Nano* **2**, 1437 (2008)

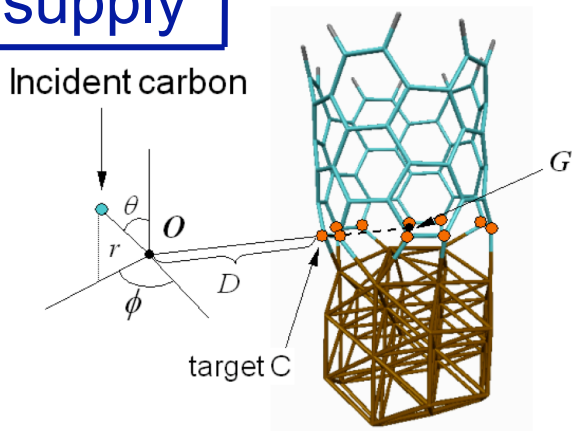

● : target candidates

G : center of mass of target candidates

(1) Target C is randomly selected from the target candidates.

(2) Point O is an extension of the line which is determined from the positions of the target C and G

(3) Incident C is randomly distributed around the point O using polar coordinates

(4) r and D are set to be 3 Å and 5 Å, respectively.

Simulation Flow Chart

T_n = 1500 K = 1227°C
Nose-Hoover chain
Δt=1 fs
velocity Verlet

Equilibrated for 10 ps

↓

10 geometries are randomly sampled between 5 and 10 ps

↓

One C atom is supplied around the C-Fe interface every 0.5 ps, incident velocity corresponding to T_n

45 ps, 90 C's are added

Y. Ohta, Y. Okamoto, SI, K. Morokuma, *ACS Nano* **2**, 1437 (2008) & *J. Phys. Chem. C*, **113**, 159, (2009)

DFTB/MD simulation

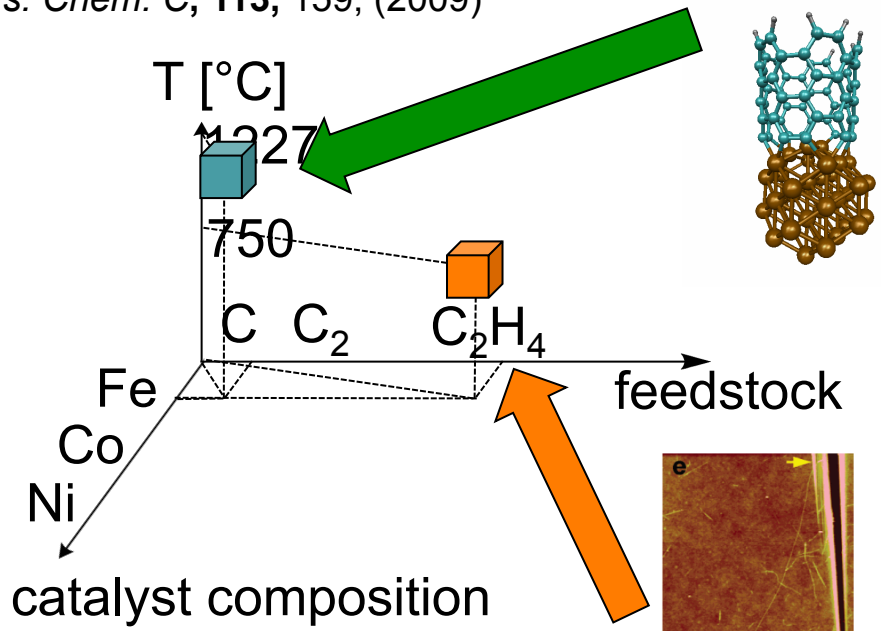

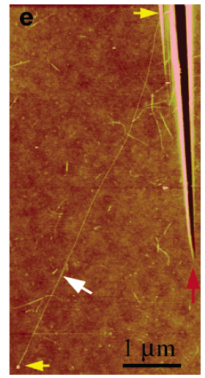

Smalley's experiment

List of theoretical "crutches":

- Targeted C **atom shooting** to Fe/C region
- **Small Fe** nanoparticle (~0.7 nm)
- **Very fast** C atom supply

All-carbon simulations — Continued Growth

Y. Ohta, Y. Okamoto, SI, K. Morokuma, *ACS Nano* **2**, 1437 (2008)

10 Trajectories after 45 ps C supply

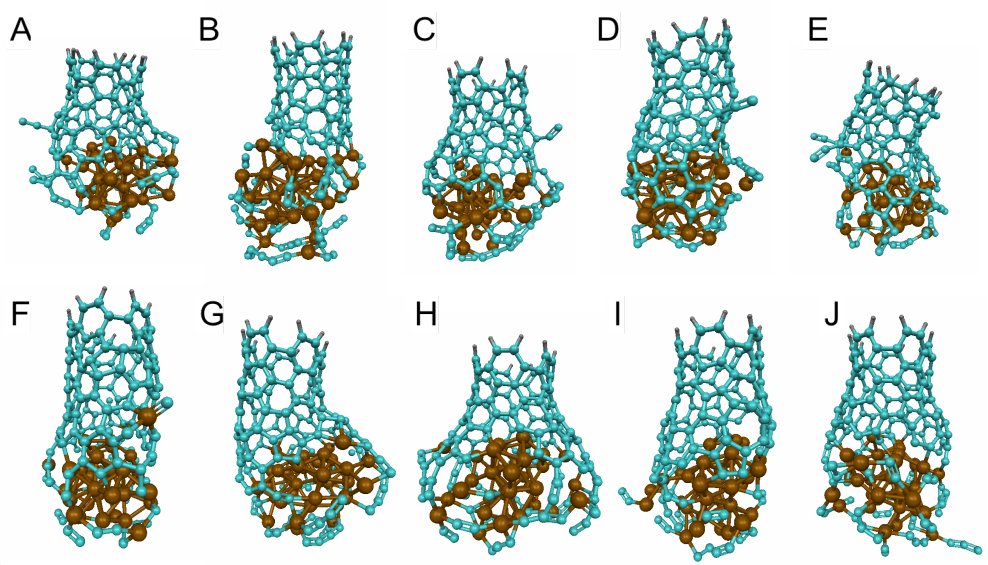

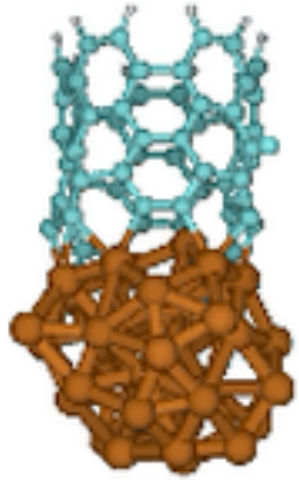

Schematic depiction of C atom insertion events

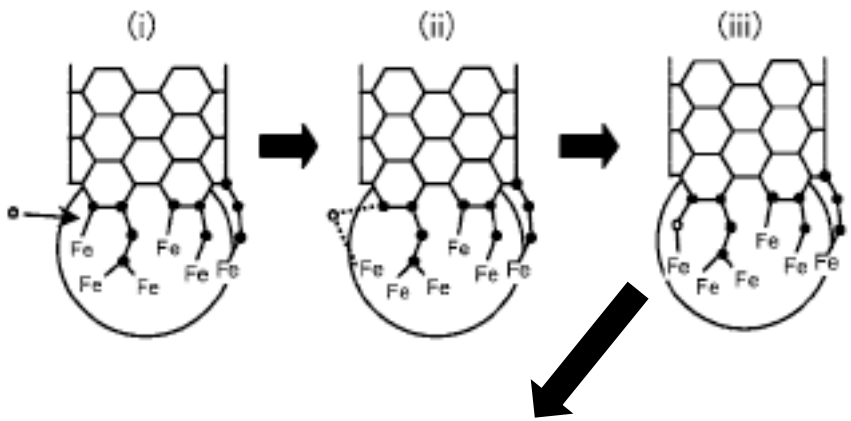

new 5-, 6-, 7-membered rings

Trajectory F

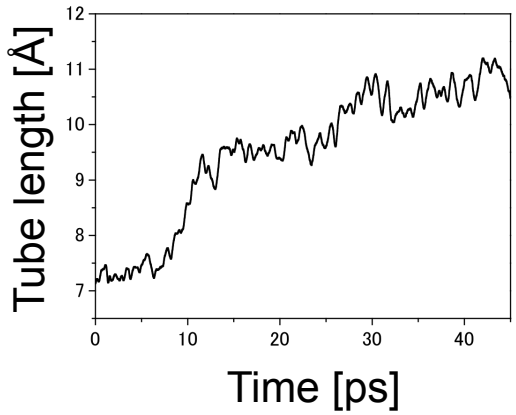

Growth rate: ~10 pm/ps

Self-healing process of sidewall (annealing)

Fe-Carbon mobility at interface important!

Trajectory 6: T_n= 1500 K, T_e = 10k K, C_{int}=1500 K

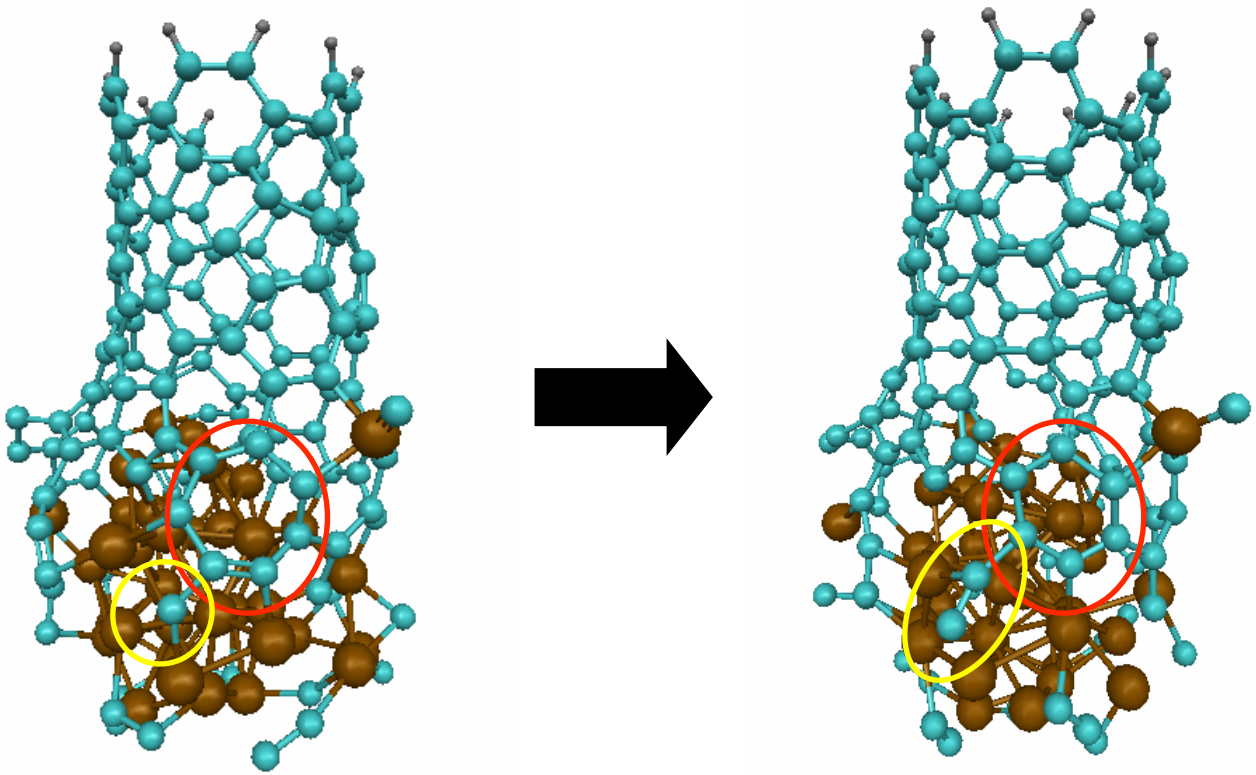

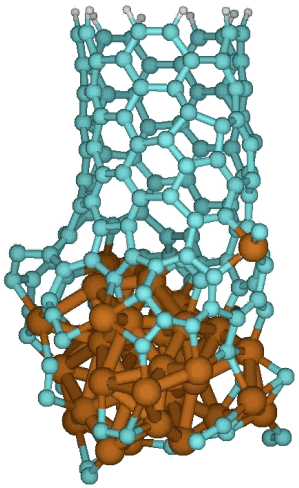

Movie

24.5 ps - 27.5 ps

Heptagon + C changes into hexagon + C_2

F. Ding, *et al. Appl. Phys. Lett.* **88**, 133110 (2006)

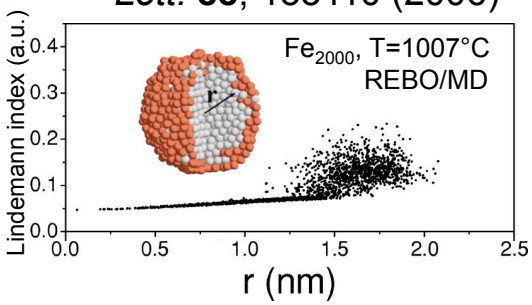

Relationship between ring type and length

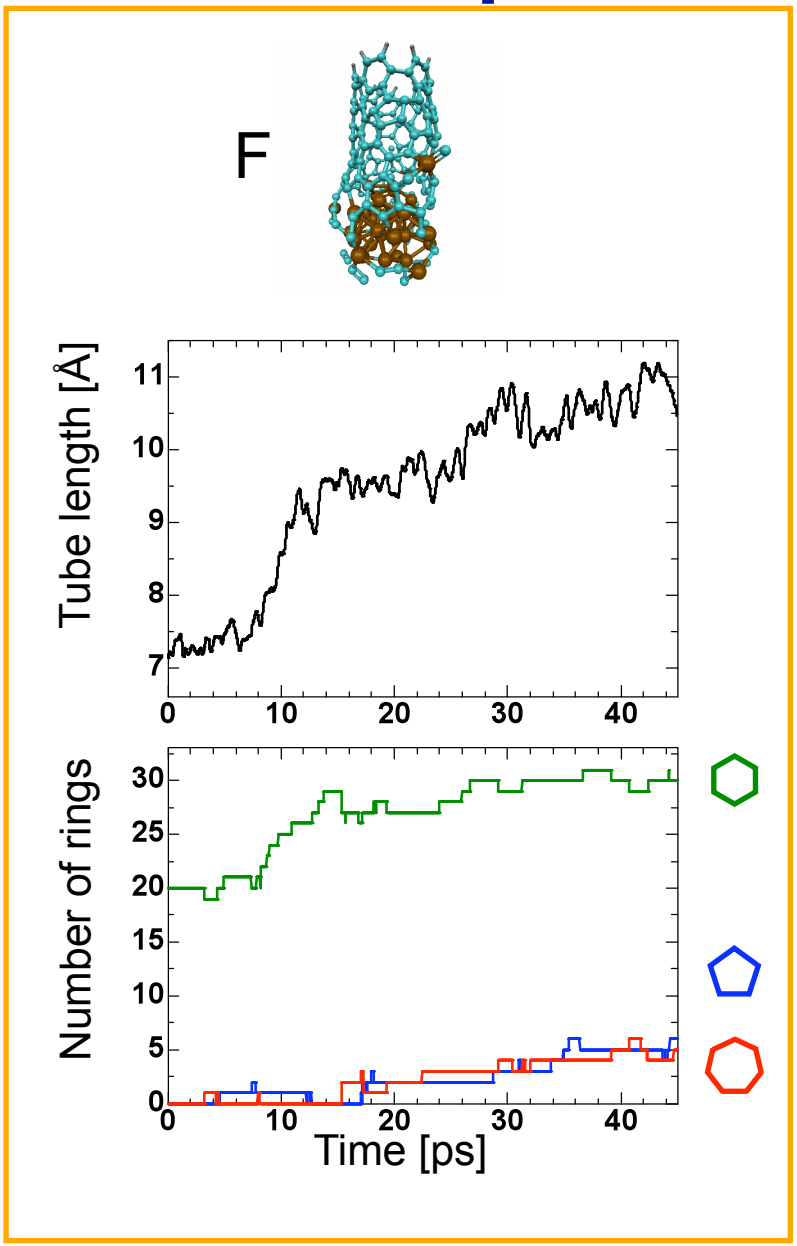

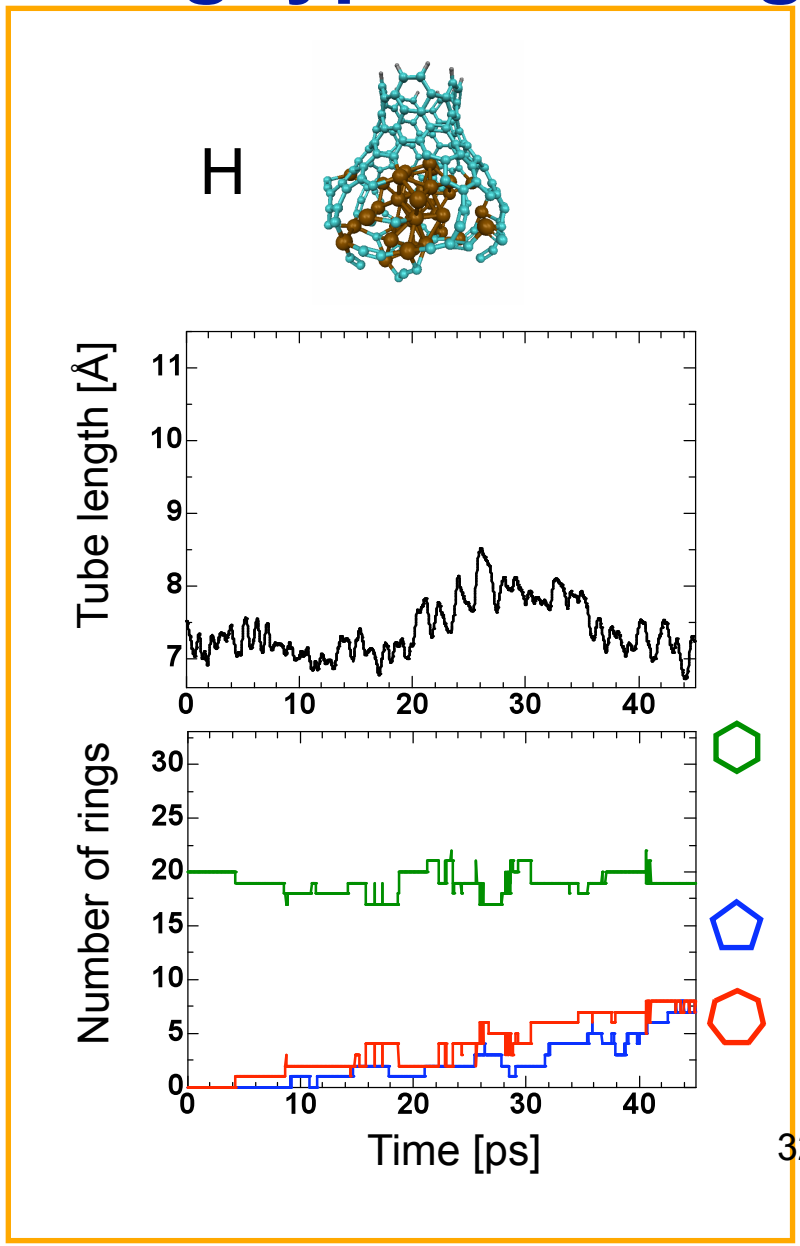

Continued SWNT growth as function of temperature ((5,5) armchair SWNT)

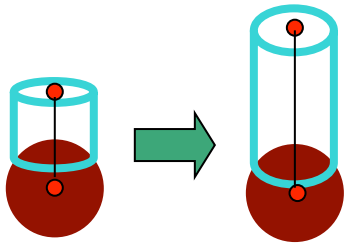

10 Trajectories for 3 temperatures

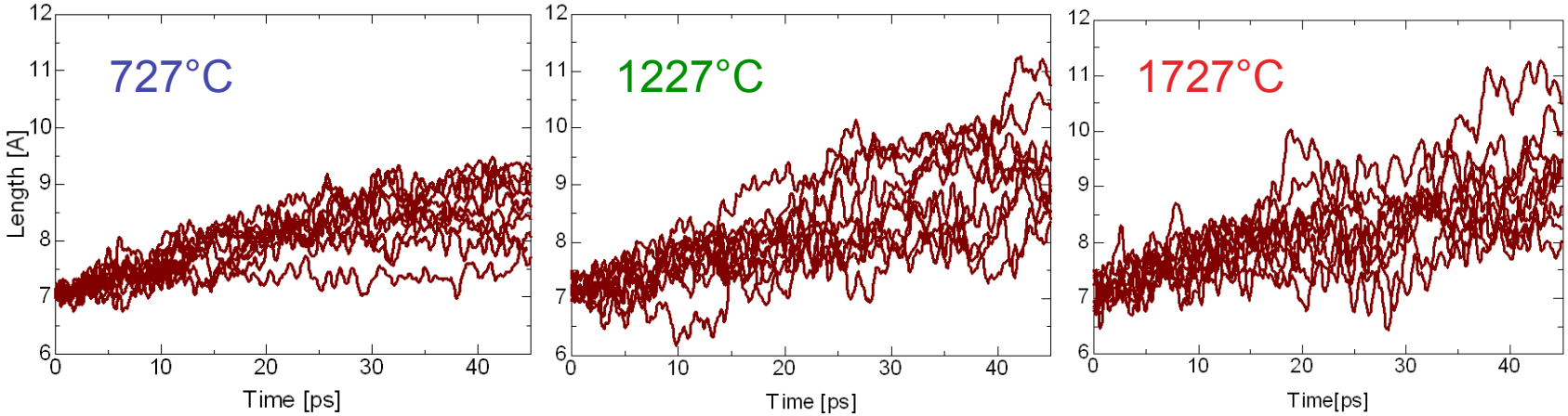

T[°C]	727	1227	1727
Growth rate [pm/ps][a]	3.48	5.07	4.13
Chain carbons[a]	3.9	0.3	0.2
SWNT C atoms[a]	112.9	110.1	102.7

[a]averaged over 10 trajectories/T

Y. Ohta, Y. Okamoto, SI, K. Morokuma, *J. Phys. Chem. C*, **113**, 159, (2009).

T=727°C

10 Trajectories after 45 ps

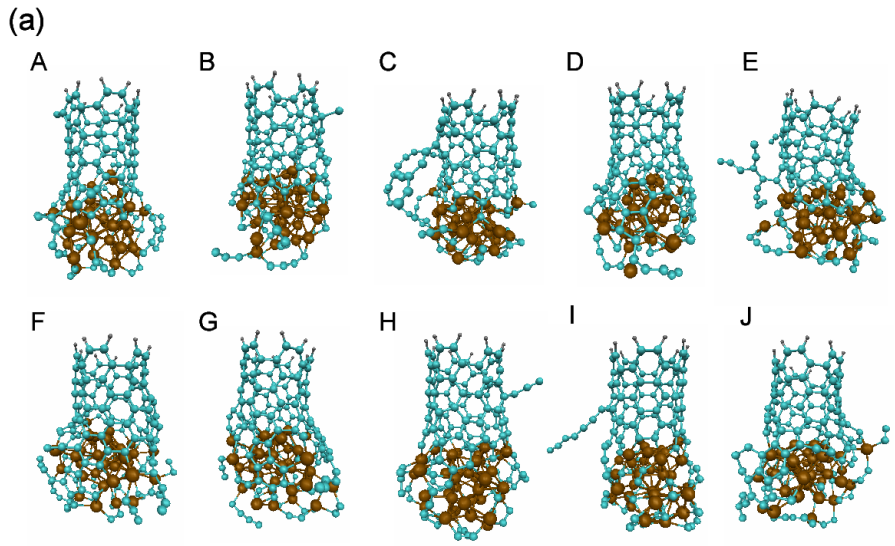

(b) Encapsulation of Fe by polyyne

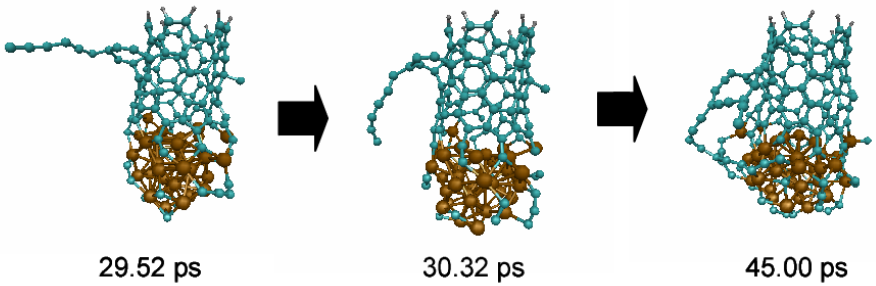

Trajectory C

T=1727°C

(a) 10 Trajectories after 45 ps

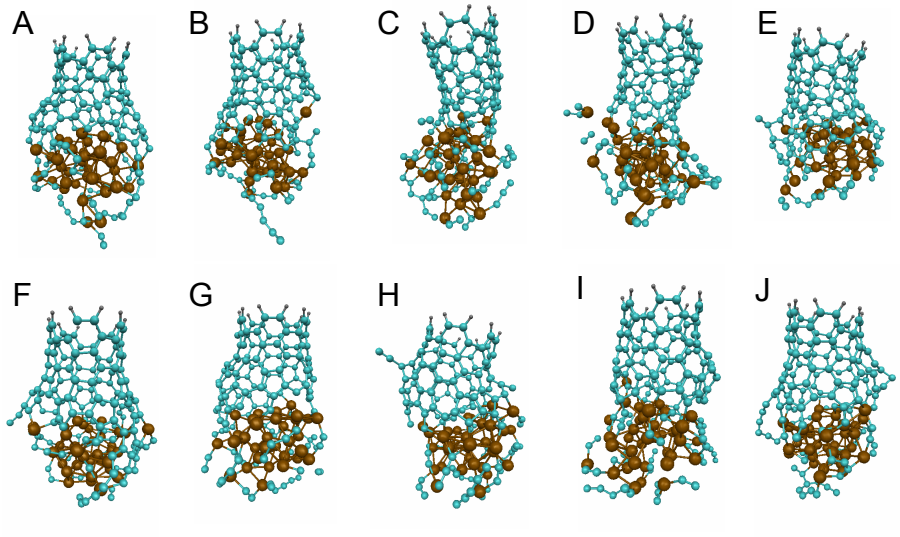

(b) Dissociation of C_2 from Fe/C

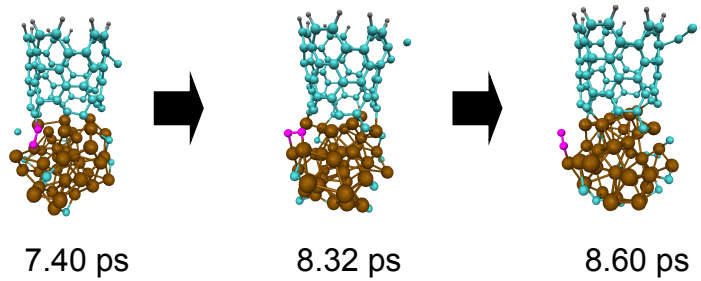

Trajectory G

Y. Ohta, Y. Okamoto, SI, K. Morokuma, *J. Phys. Chem. C,* **113**, 159, (2009).

Using (8,0) seed SWNT

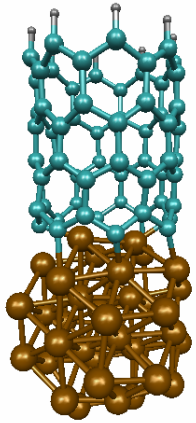

(8,0) zigzag

length = 7.1 Å

diameter = 6.3 Å

fcc Fe_{38}

$H_{10}C_{62}Fe_{38}$

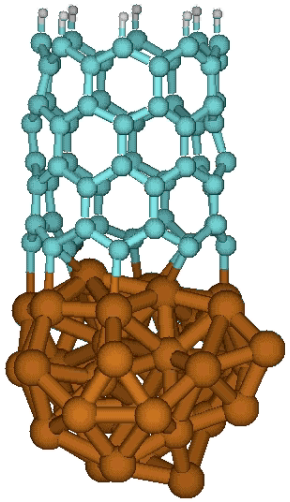

Equilibrated at 1500 K

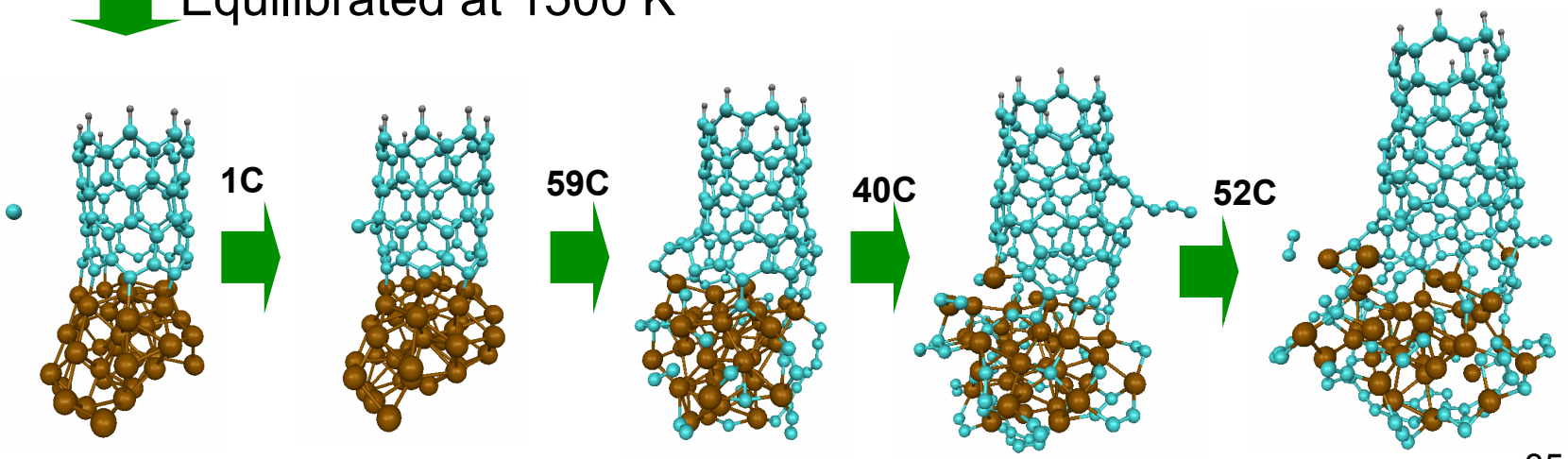

0.0 ps 0.5 ps 30.0 ps 50.0 ps 76.0 ps

Cap Fragment Formation DFTB/MD Annealing

Y. Ohta, Y. Okamoto, A. J. Page, SI, K. Morokuma, ACS Nano **3**, 3413 (2009)

Initial model: Fe_{38}

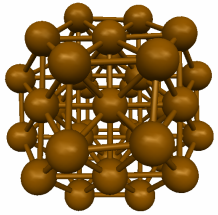

10 ps

Annealed at 1500 K

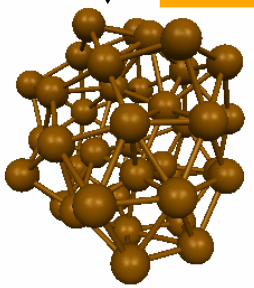

30 C_2's

30 ps

t = 0 ps

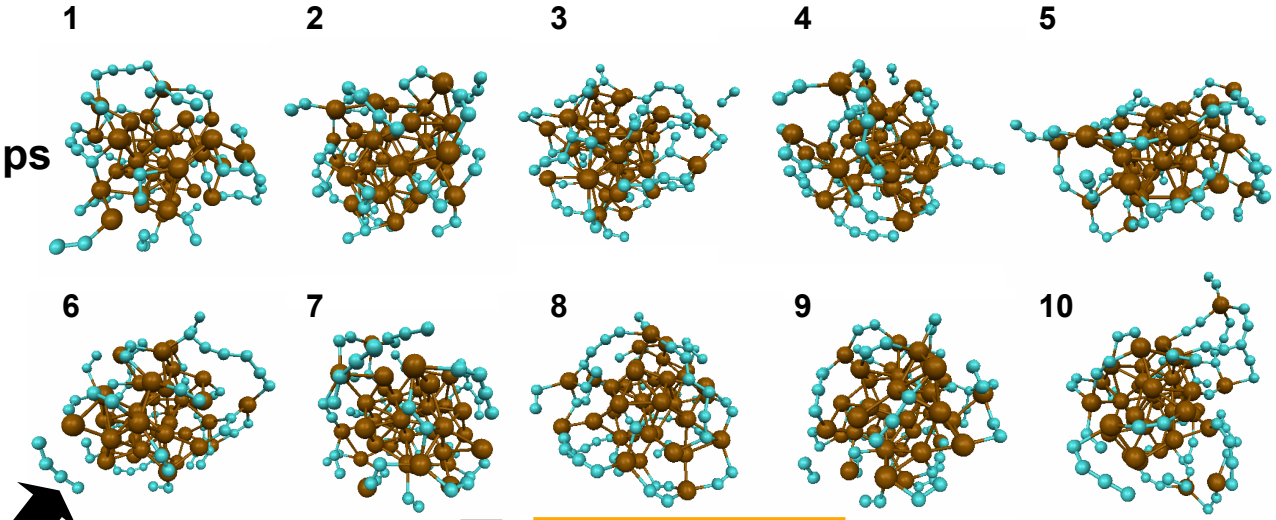

410 ps

Annealed at 1500 K

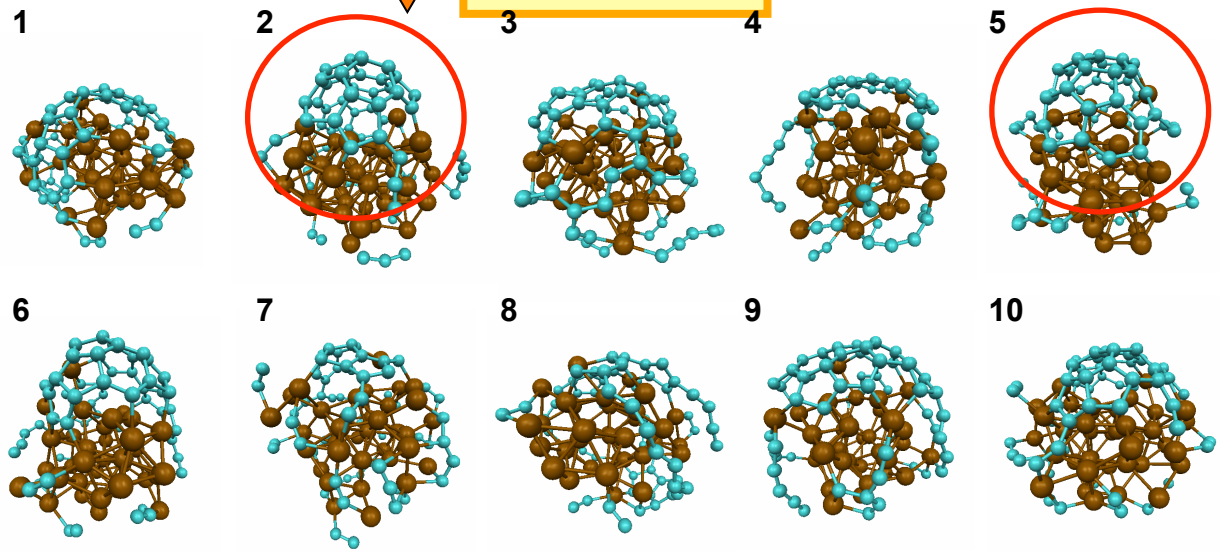

t = 410 ps

10 geometries are randomly sampled between 5 and 10 ps for ten trajectories.

Cap Fragment Formation DFTB/MD Annealing

Y. Ohta, Y. Okamoto, A. J. Page, SI, K. Morokuma, ACS Nano **3**, 3413 (2009)

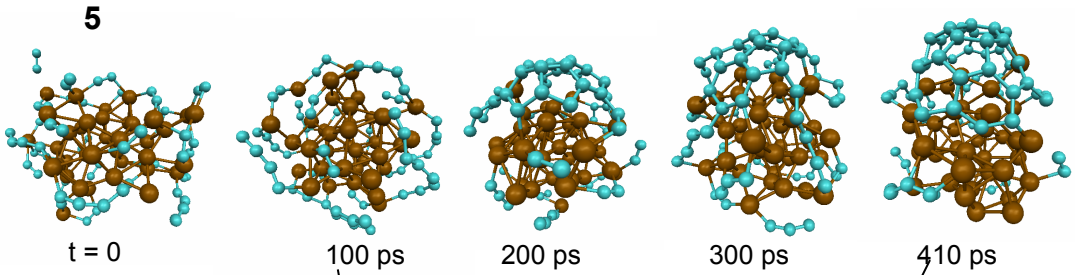

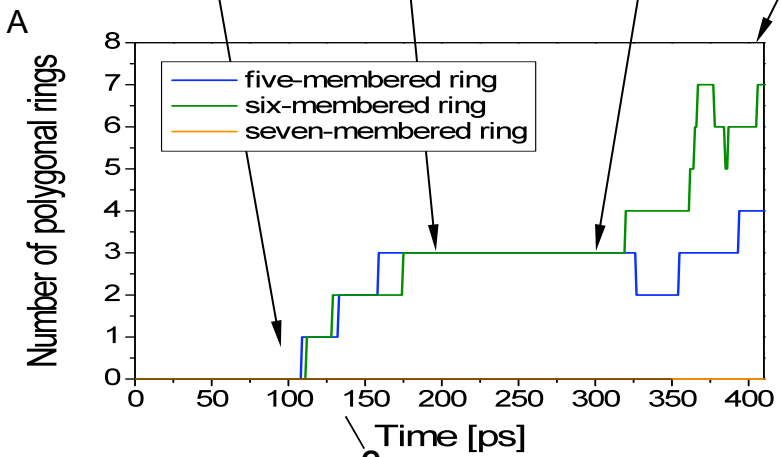

Average 5- and 6-ring counts over 10 annealing trajectories

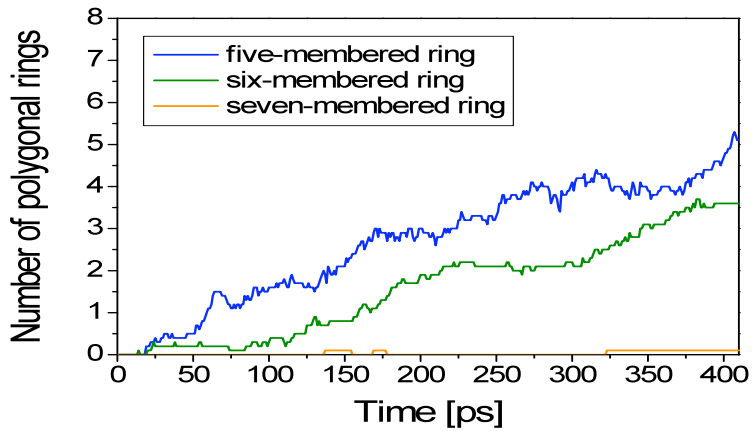

Formation of first condensed 2-ring system (5/5 or 5/6)

Always pentagon first!

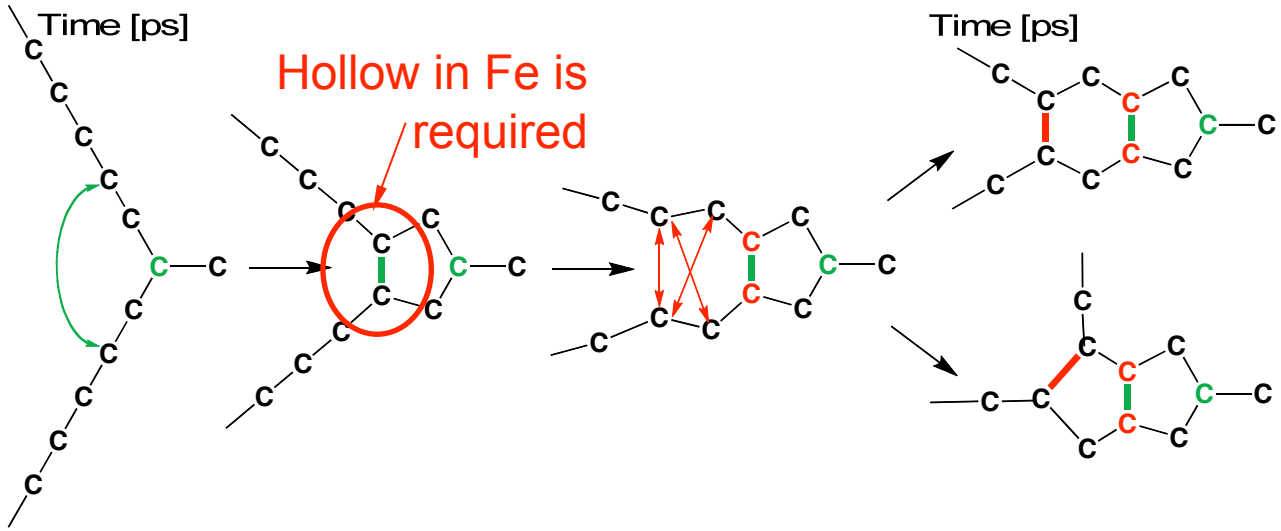

Cap Fragment Formation DFTB/MD Annealing

Y. Ohta, Y. Okamoto, A. J. Page, SI, K. Morokuma, ACS Nano **3**, 3413 (2009)

5

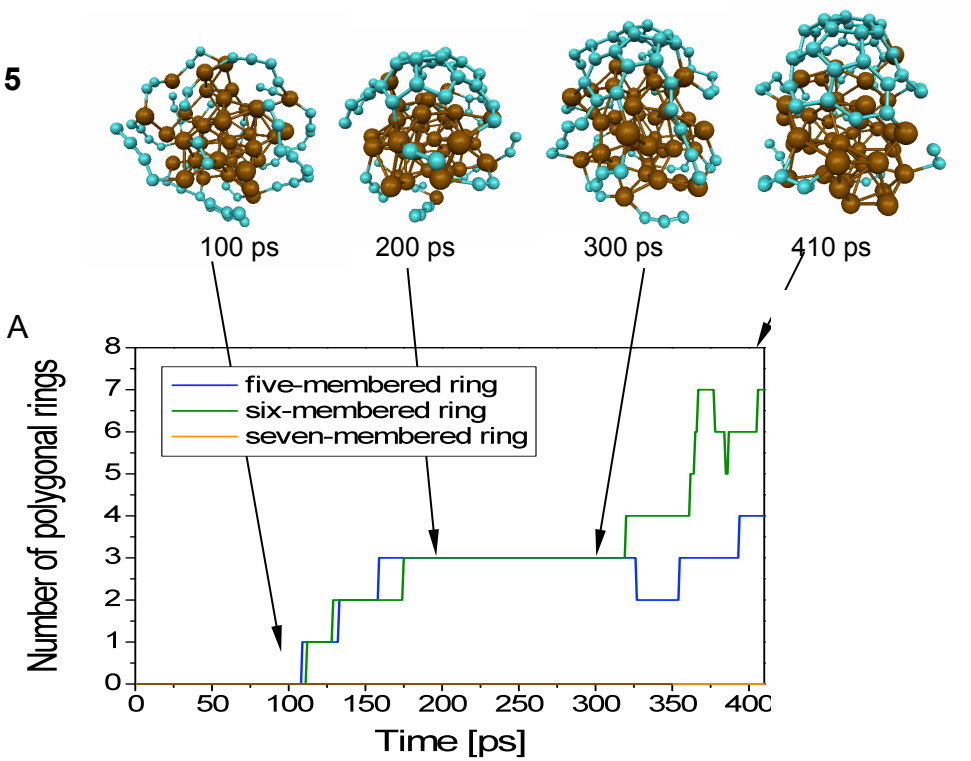

Movie, **5**

Δt(frames)=2ps

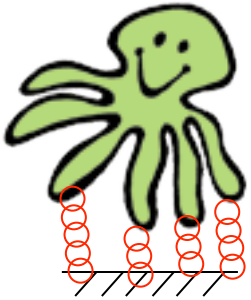

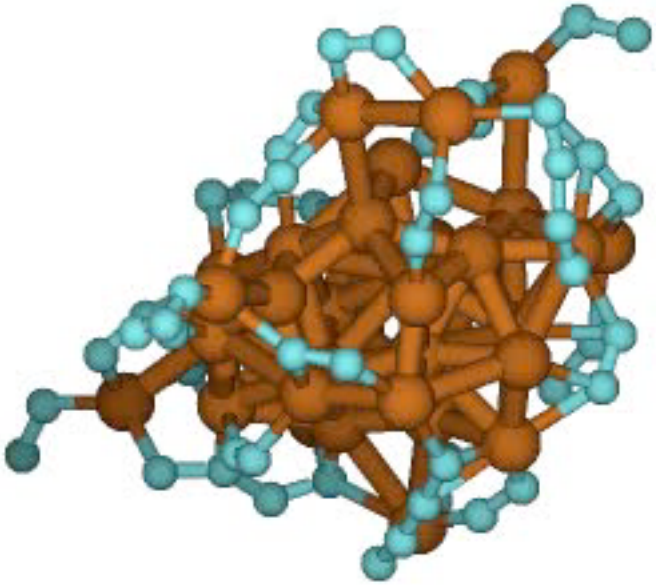

Surface Diffusion DFTB/MD Annealing

Y. Ohta, Y. Okamoto, SI, K. Morokuma Carbon **47**, 1270 (2009)

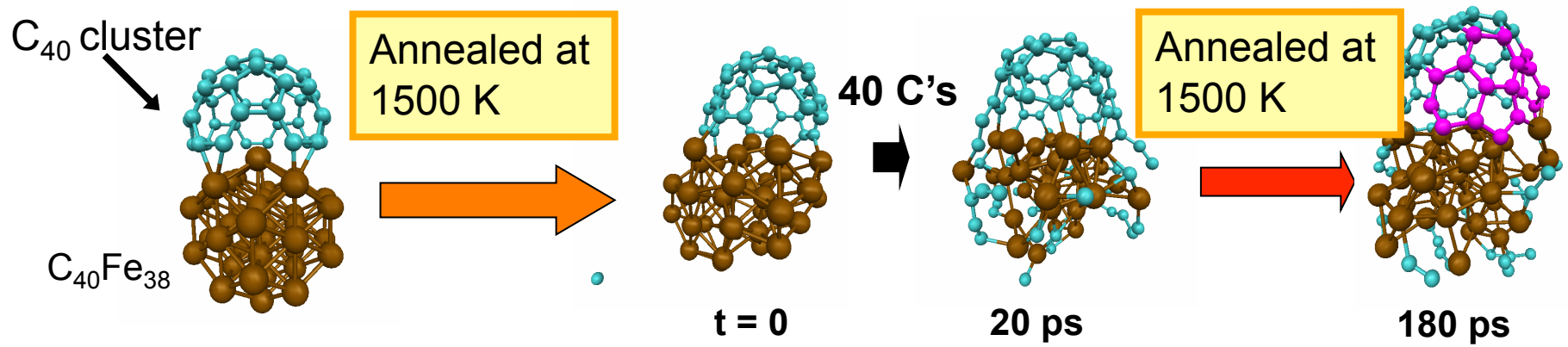

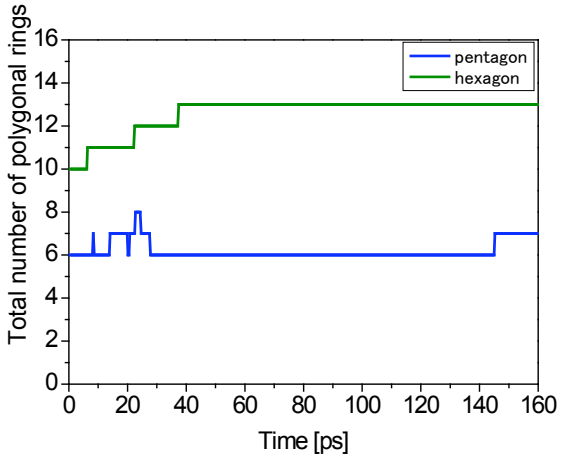

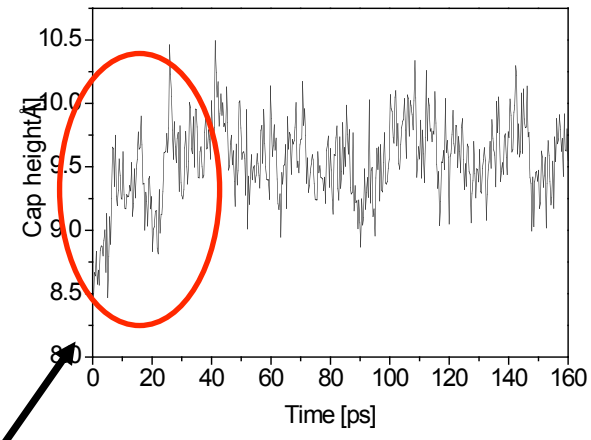

Time variation of the averaged number of rings

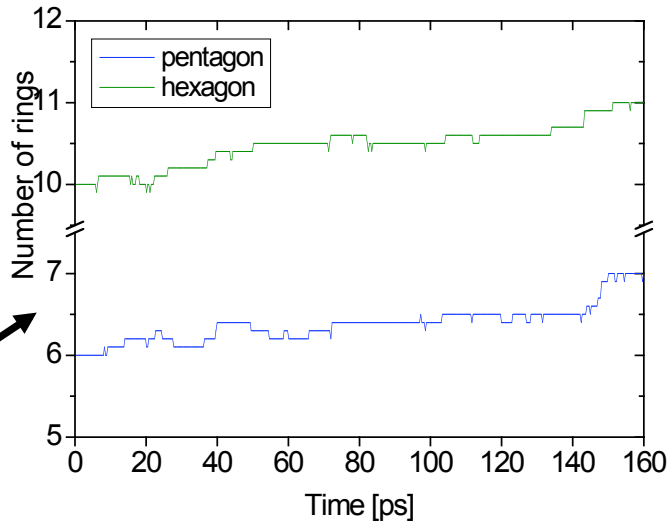

Lift-off of cap cluster was observed

Only pentagons and hexagons were formed

Cap Growth

DFTB/MD

Y. Ohta, Y. Okamoto, SI, K. Morokuma, Phys. Rev. B **79,** 195415 (2009)

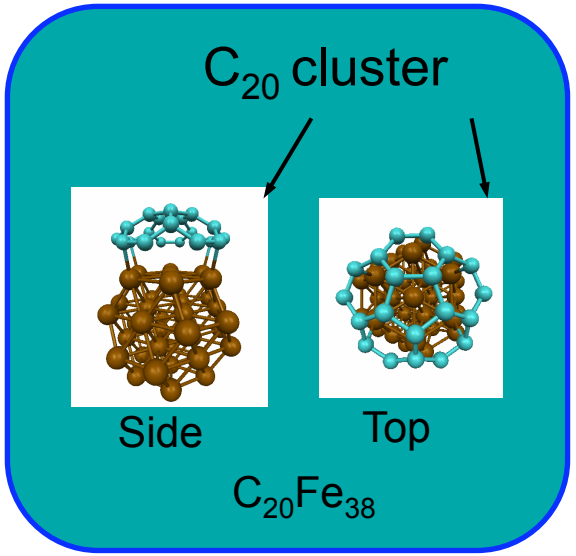

Experimental snaphots

H. Yoshida et al, Nano Lett. (2008).

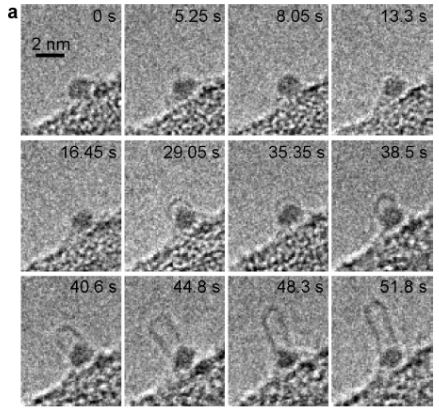

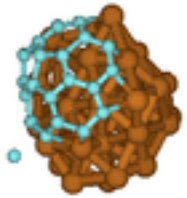

Nanotube 10 Å long was formed.

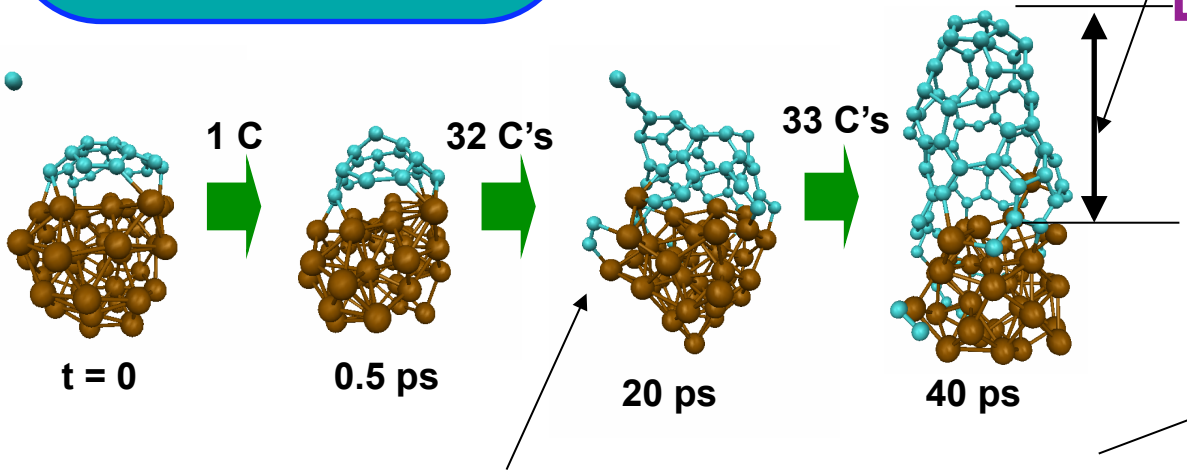

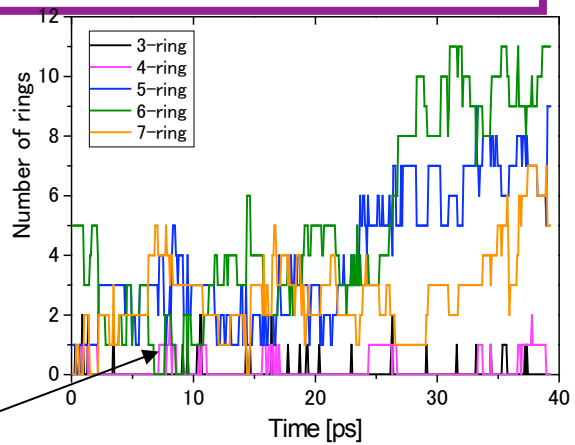

During growth, non-hexagonal rings and polyyne chains frequently formed and then rearrangement of sp^2 network occurs to construct carbon sidewall.

Outline

- Review: Experiments and previous theoretical modeling
- Density-functional tight-binding (DFTB) method
- All-carbon cap nucleation and growth on iron particles
- **Comparison of growth mechanisms between iron and nickel catalysts**
- Simulation of early stages during ACCVD (C_2H_2 and OH on iron catalyst)
- Summary and outlook

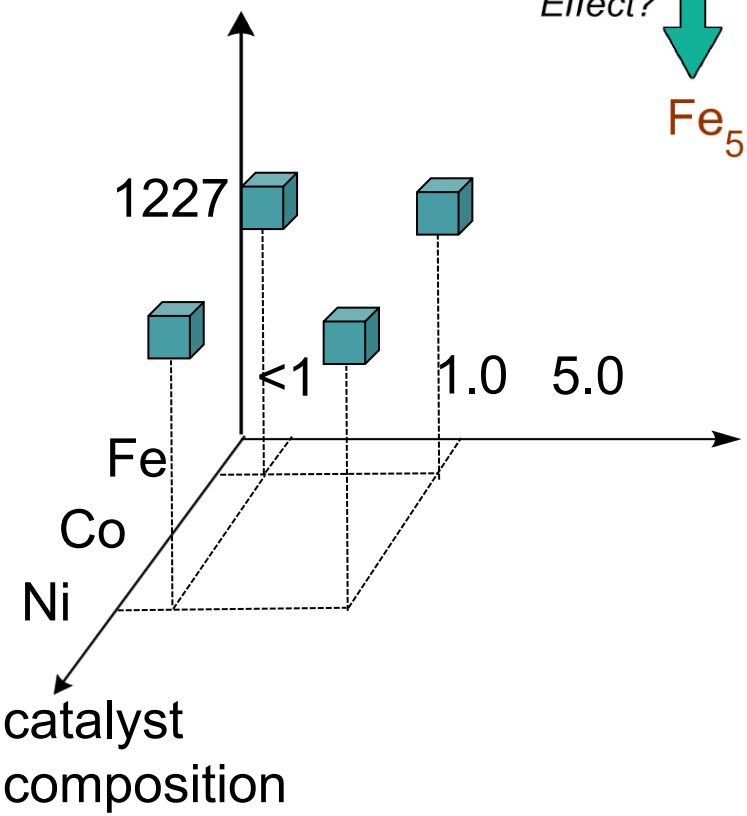
T [°C]
1227
<1
1.0
5.0
Fe
Co
Ni
catalyst composition
catalyst diameter [nm]

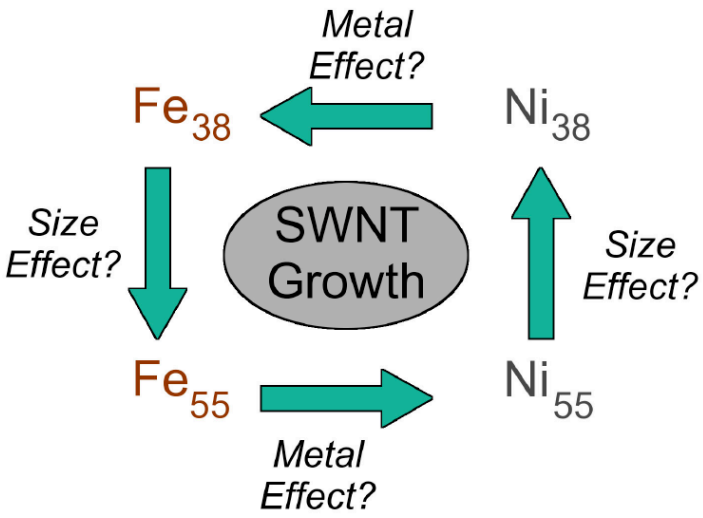
Metal Effect?
Fe38
Ni38
Size Effect?
SWNT Growth
Size Effect?
Fe55
Ni55
Metal Effect?

Comparison of $M_{38}C_{40}$+nC and $M_{55}C_{40}$+nC Growth

Adhesion energies x 10 [eV]

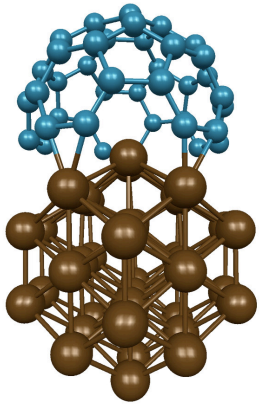

C_{40}-Fe_{38}
-1.78

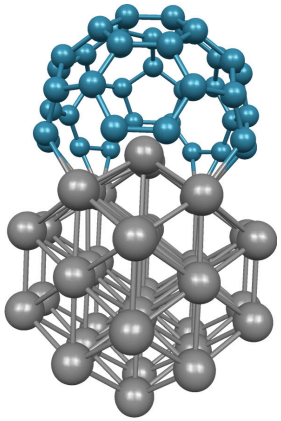

C_{40}-Ni_{38}
-1.07

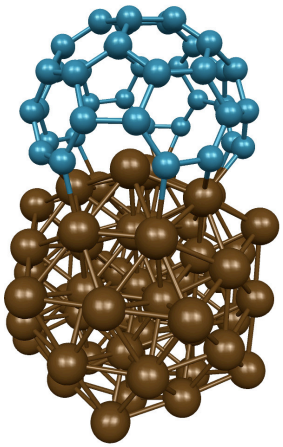

C_{40}-Fe_{55}

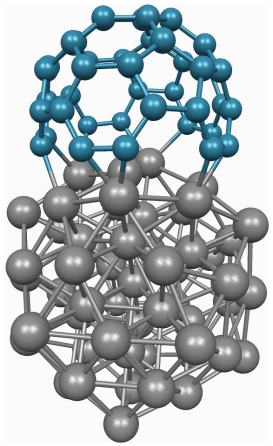

C_{40}-Ni_{55}

Cap growth methodology:

- SCC-DFTB/MD
- MD: T_n= 1500 K, T_e = 10,000 K, Δt=1 fs
- Velocity-Verlet integration
- Nosé-Hoover chain thermostat
- All trajectories replicated x 10

- Carbon supplied to Cap-M_x boundary.
- Carbon supplied @ 1 C / 0.5 ps ("fast") and @ 1 C / 10 ps ("slow")

"Fast" growth on $M_{55}C_{40}$+nC: M=Fe

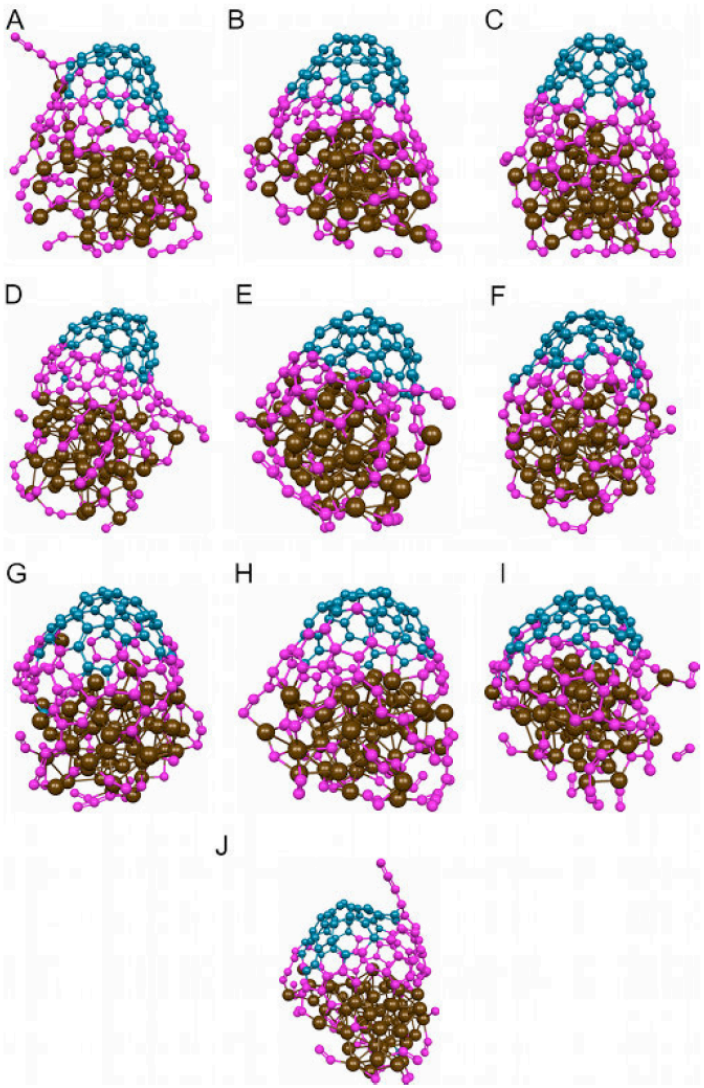

Trajectory C_{Fe}

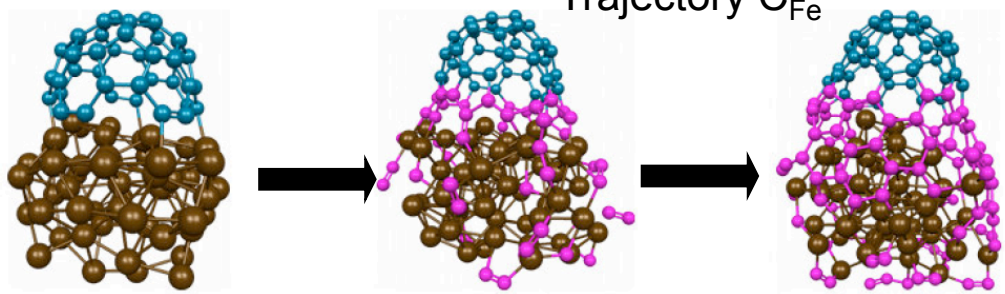

0 ps 25 ps, 50 C's 50 ps, 100 C's

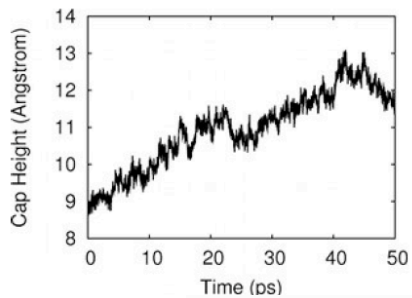

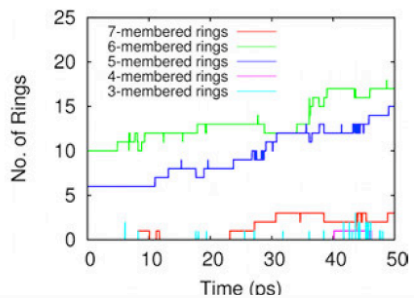

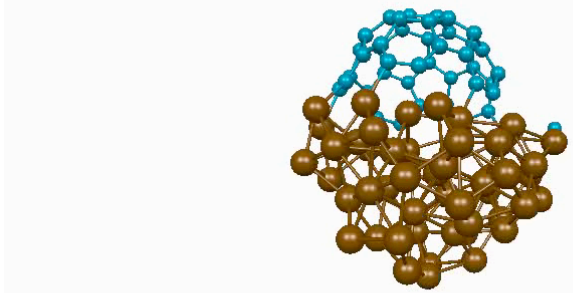

A. Page, S. Minami, Y. Ohta, SI, K. Morokuma, submitted

"Fast" growth on $M_{55}C_{40}$+nC: M=Ni

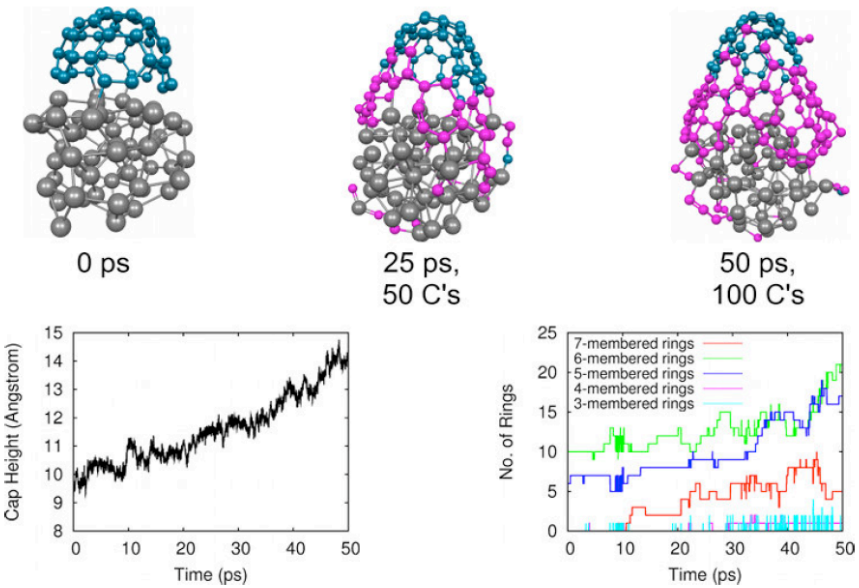

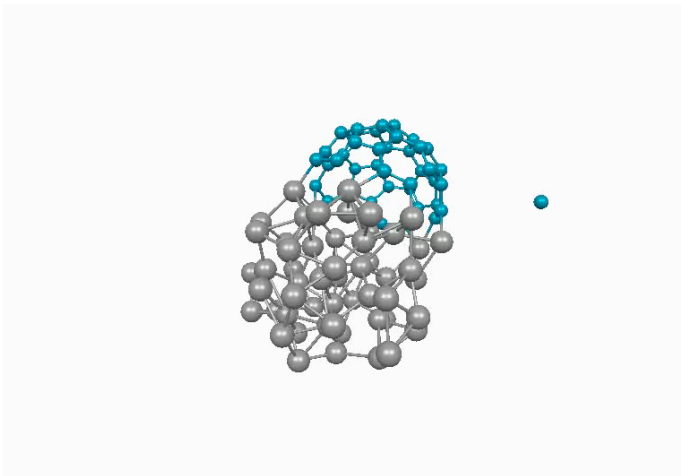

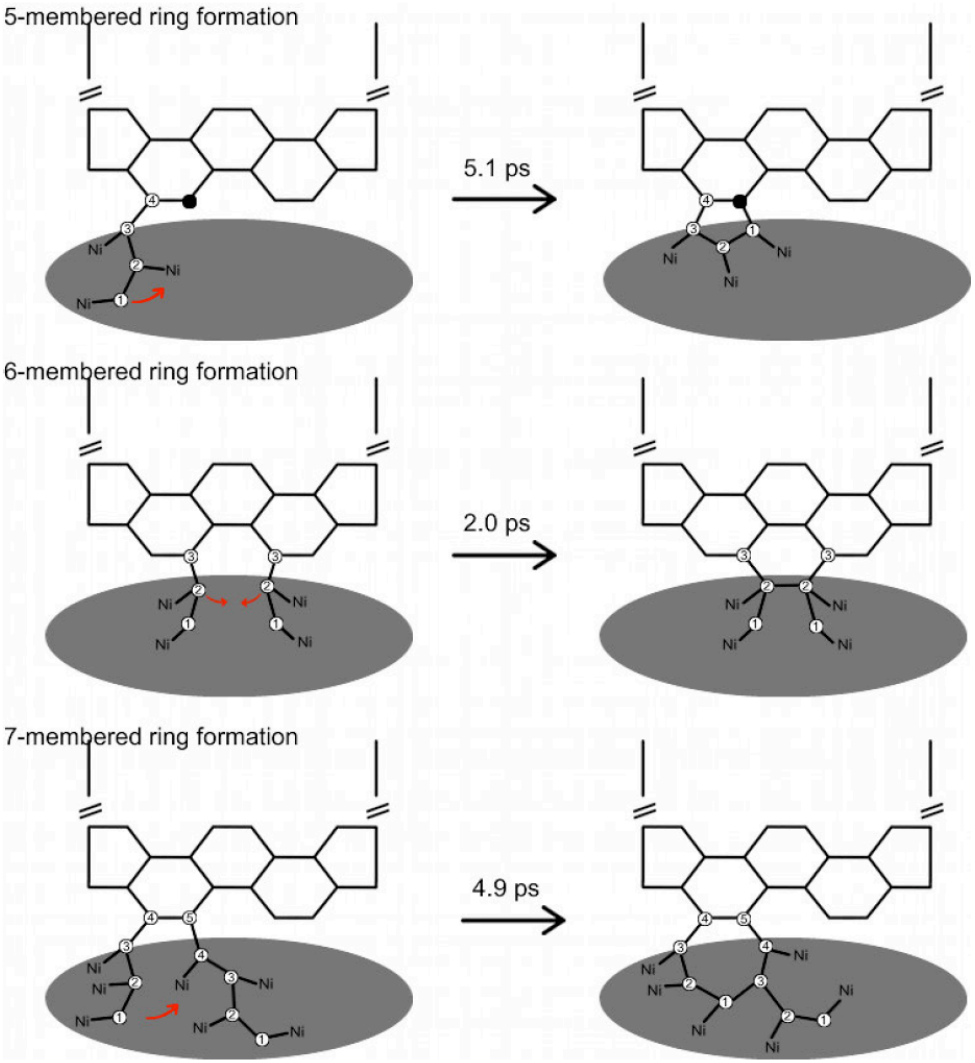

(Ni_{55}-catalyzed SWNT, Trajectory I)

A. Page, S. Minami, Y. Ohta, SI, K. Morokuma, submitted

Comparison of $M_{55}C_{40}$+nC

Average Growth and Ring Addition Statistics:

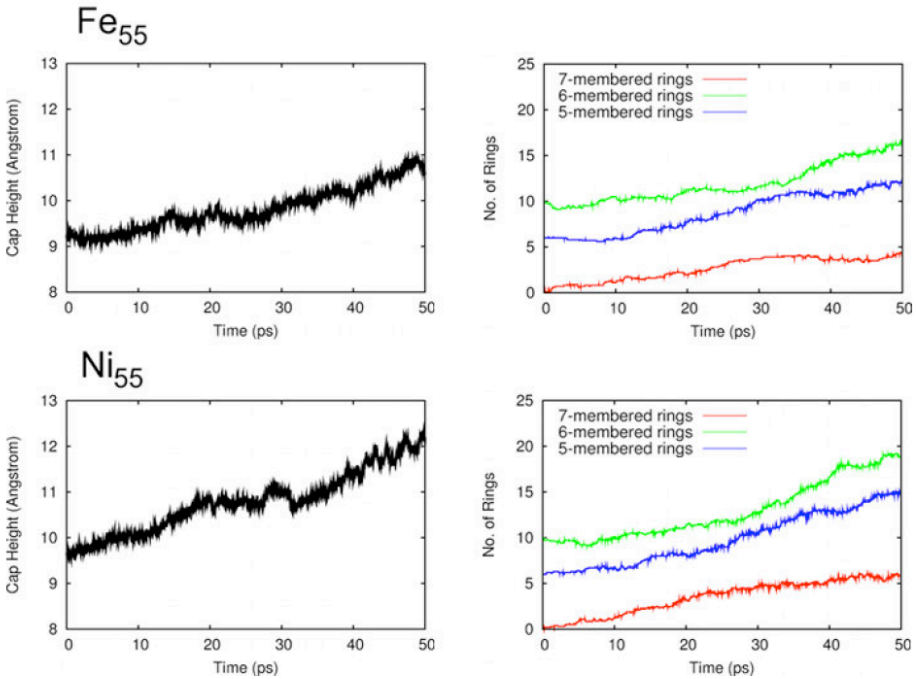

Metal Effect: Average Fe_{55}- & Ni_{55}-Catalyzed Growth Statistics

	Fe_{55}	Ni_{55}	Fe_{55}:Ni_{55} Ratio
5-m rings added	6.2	9.0	1:1.45
6-m rings added	6.5	9.0	1:1.38
7-m rings added	4.4	5.9	1:1.34
Growth Rate (dÅ/ps)	2.88	4.87	1:1.69

A. Page, S. Minami, Y. Ohta, SI, K. Morokuma, submitted

Correlation with Stability of $Ni_{55}-C_n$ Chains:

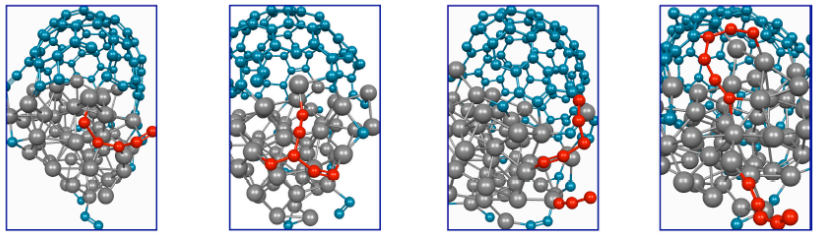

21.6 ps 25.0 ps 34.2 ps 40.0 ps

Corresponding Behaviour of M_{55} Catalysts:

$$\Delta_B = \frac{2}{N(N-1)} \sum_{i<j} \frac{\sqrt{\langle \Delta r_{ij}^2 \rangle}}{\langle \Delta r_{ij} \rangle}$$

Zhou *et al.*, *JCP*, **116**, 2323, (2002).

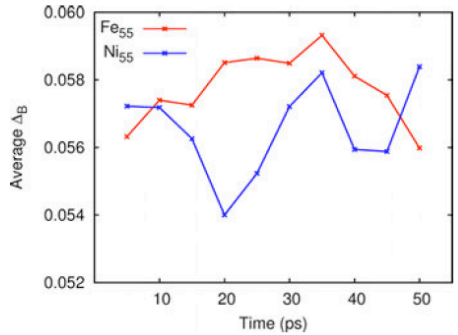

$\Longrightarrow$ **SWNT growth rate increases using Ni_{55}, compared to Fe_{55}.**

(Experiment: Ni-catalysts decompose feedstock (CH_4) faster than Fe-catalysts...)

Mora & Harutyunyan, *JPCC*, **112**, 4805, (2008).
Ermakov *et al.*, *Catal. Today*, **77**, 225, (2002).

Size Effect: $M_{38}/M_{55}C_{40}$+nC

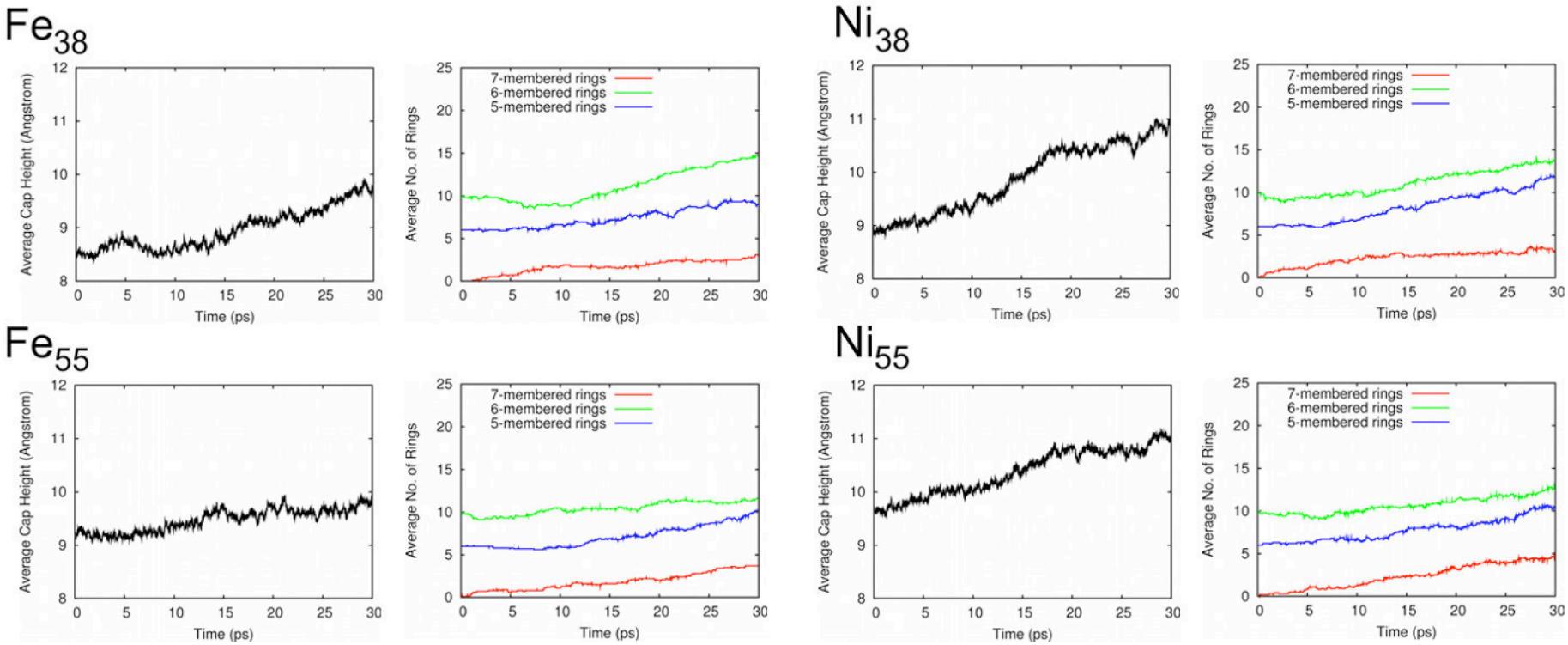

Size Effect: Average Growth (Average Growth Rates, dÅps^{-1}) using M_x Catalysts after 30 ps

	M=Fe	M=Ni
$x = 38$	1.229(4.10)	1.961(6.53)
$x = 55$	0.654(2.18)	1.302(4.34)
M_{38}:M_{55}	1.88:1	1.51:1

$\Longrightarrow$ **SWNT growth rate decreases with increasing catalyst size.**

Larger catalyst particle $\Longrightarrow$ greater surface area + volume for the decomposed carbon to explore before contributing to the SWNT base.

A. Page, S. Minami, Y. Ohta, SI, K. Morokuma, submitted

Summary: Cap growth on M_x

- SWNT growth simulated using M_x catalysts (M = Fe, Ni; x = 38, 55).
- Effect of catalyst composition and size determined.
- Correlations between SWNT growth rate/mechanism and TM-C adhesion energies observed.
- Ni-catalyzed SWNT growth mechanism established using QM/MD.

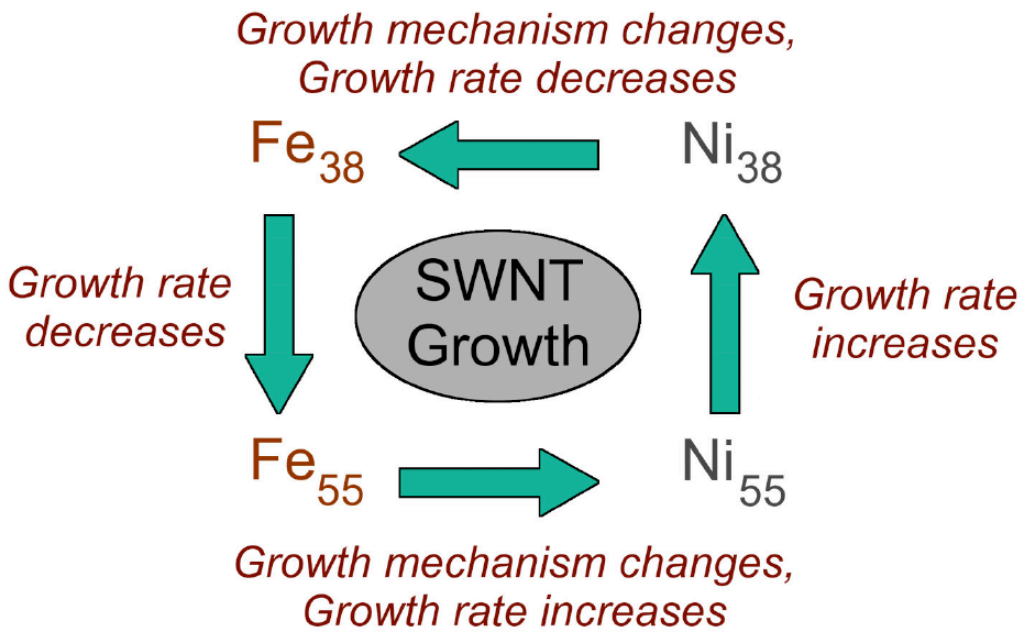

A. Page, S. Minami, Y. Ohta, SI, K. Morokuma, submitted

Outline

- Review: Experiments and previous theoretical modeling
- Density-functional tight-binding (DFTB) method
- All-carbon cap nucleation and growth on iron particles
- Comparison of growth mechanisms between iron and nickel catalysts
- **Simulation of early stages during ACCVD (C_2H_2 and OH on iron catalyst)**
- Summary and outlook

Active Species: C_2H_2, OH

$C_2H_5OH \rightarrow C_2H_4 + H_2O$
$C_2H_4 \rightarrow C_2H_2 + H_2$

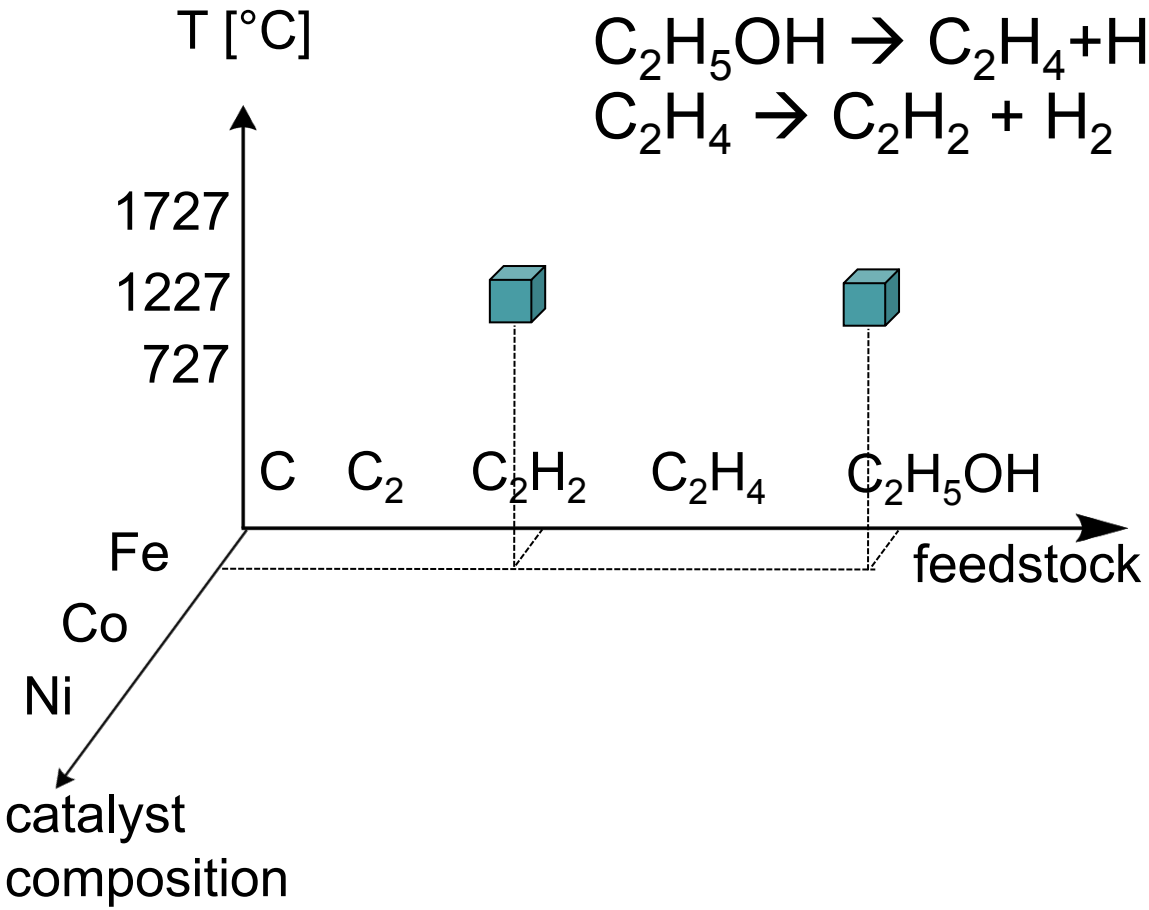

Acetylene CVD

Polymerization

Initial model: Fe_{38}

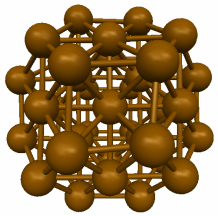

t = 0 ps

10 ps

Annealed at 1500 K

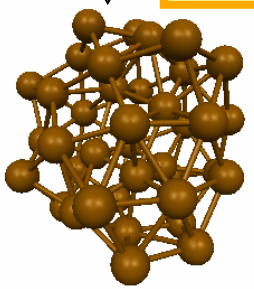

30 C_2H_2's

30 ps

10 geometries are randomly sampled between 5 and 10 ps for ten trajectories.

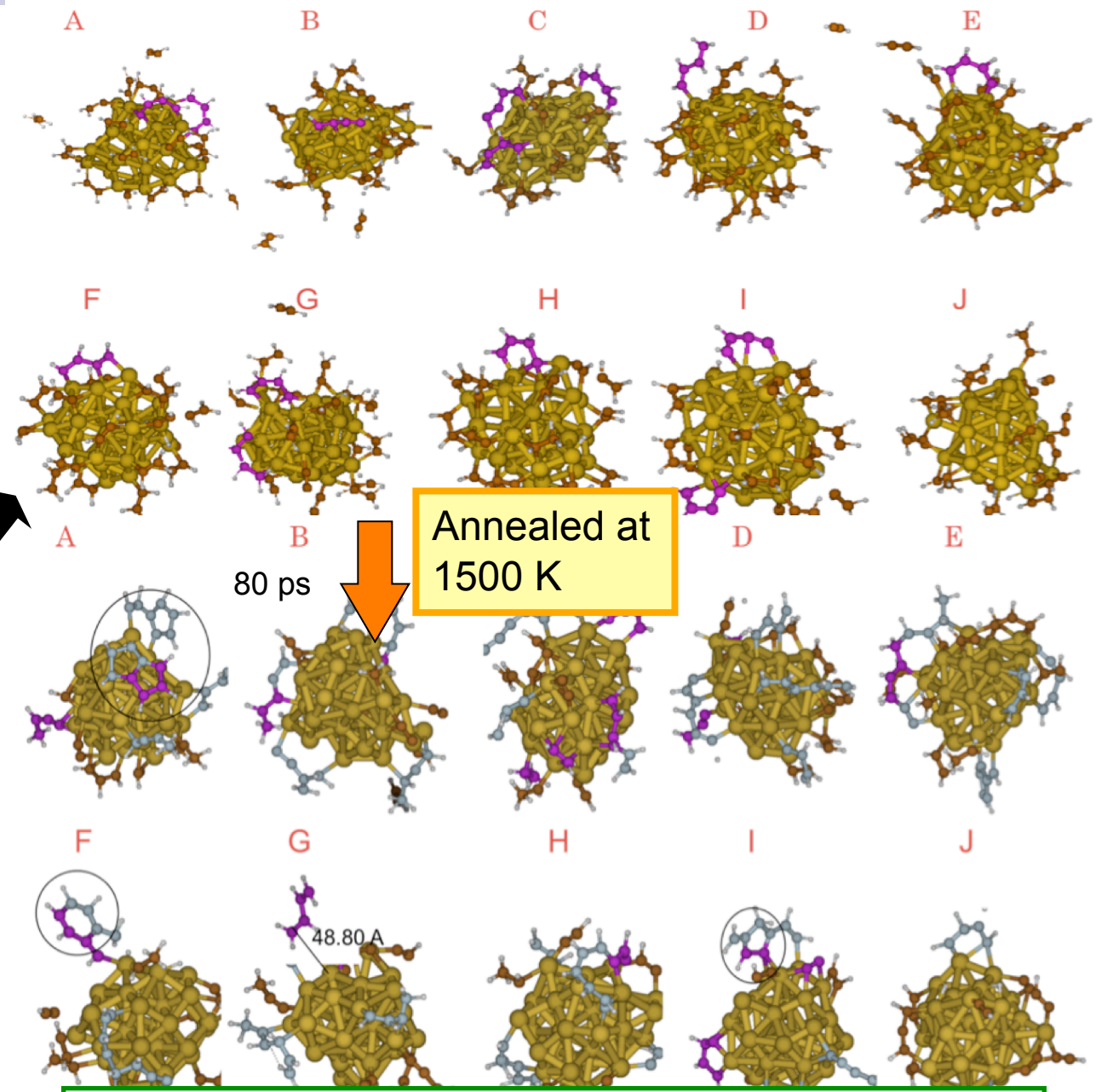

Polyacetylene formation, largest carbon cluster: $C_{10}H_x$

C-C Bond formation

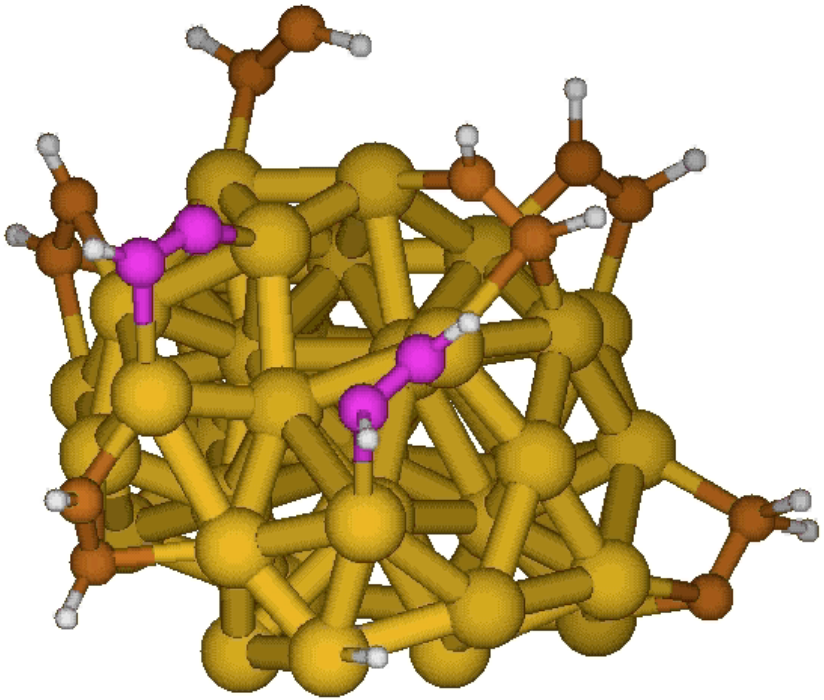

C-C Bond formation:

$C_2H_2(ads)+C_2H(ads) \rightarrow C_4H_3(ads)$

Relative energies in [kcal/mol]
Including ZPE
IRC verified
Using GAUSSIAN external

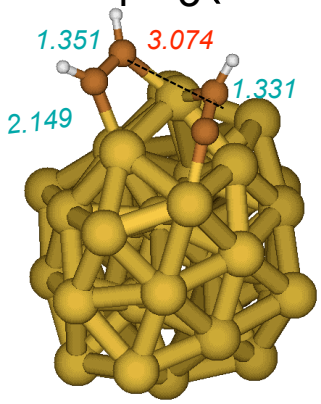

0.0

NImag=0

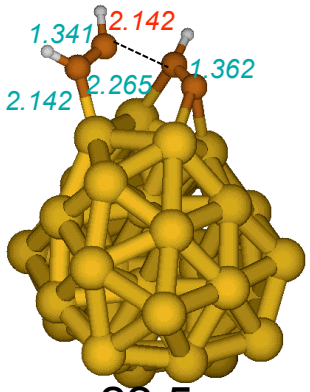

22.5

NImag=1

ν_{imag}= 455i cm^{-1}

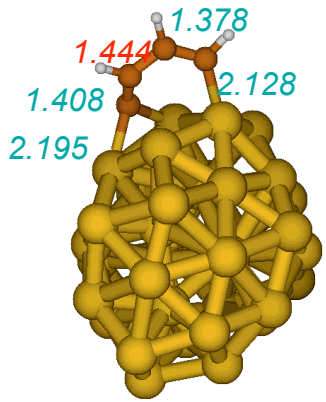

-11.8

NImag=0

H abstraction:

$C_2H_2(ads) \rightarrow C_2H\,(ads) + H(ads)$

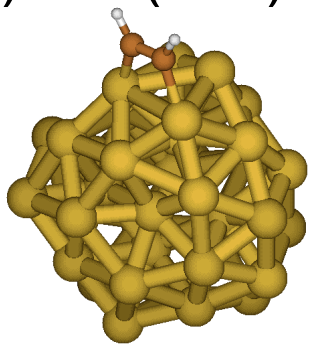

0.0

NImag=0

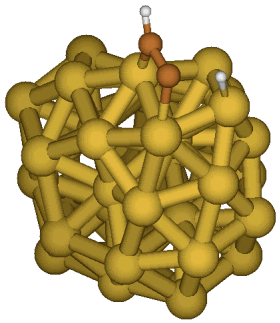

36.5

NImag=1

ν_{imag}= 1377i cm^{-1}

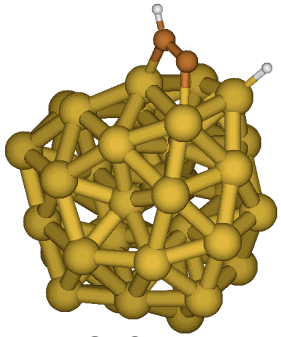

8.0

NImag=0

Acetylene CVD

Species formed

Trajectory	Last cluster	on cluster	off cluster
A	$Fe_{38}H_{33}C_{38}$	$HC_{(2)}$;C_2(1);H_5C_7(1);H_4C_4 (3);H_3C_3(1);HC_2(1);H_5C_8(1);H(1);H_4C_2 (1)	H_4C_2(2);H_2C_2 (8);H_3C_2 (1)
B	$Fe_{38}H_{26}C_{36}$	H_5C_5(1);H_3C_7(1) ;HC_2(4);H(3); C_2(3); H_4C_5(1);H_2C(1); H_5C_4 (1)	H_4C_2(5); H_2C_2 (7)
C	$Fe_{38}H_{40}C_{42}$	C_2(2);H_6C_6(1);H_2C_4(1);HC_2(2);H_2C_2(3);H_4C_2(1);H(2);H_3C2(1);H5C_2(1);H_4C_4(1);H_6C_8 (1)	H_4C_2(1);H_2C_2 (8)
D	$Fe_{38}H_{42}C_{44}$	H_5C_6(1);H_3C_3(1);H_3C_6(1);H_6C_6(1);C_2(2);H_2C_2(2);H(1);H_2C_4(1);H_4C_3(1);H_3C_2(3);H_5C_2 (1)	H_4C_2(1);H_2C_2 (7)
E	Fe_{38} $H_{42}C_{44}$	H_9C_{10}(1);H_7C_8(1);H_2C_3(1);H_3C(1);HC(1);H_2C_2(3);H_3C_2(1);H_2C_5(1);H_3C_4(1);HC_2 (1);H_5C_2 (1)	H_4C_2(1);H_2C_2 (7)
F	$Fe_{38}H_{35}C_{38}$	H_2C_2(2);C_2(2);H_3C_2(3);H_5C_2 (1);H_5C_8(1);H_7C_8(1);H_3C_4 (1);HC_2 (1);H(1)	H_2C_2(10);H_5C_2 (1)
G	Fe38H31C37	HC_2(6);H_4C_6(1);H_3C_3(2);H_8C_6(1);H(1);H_2C_3(1);H_4C_4 (1)	H_2C_2(6);H_3C_2(1);H_4C_3(1);H_6C_4(1) ;H_4C_2 (1)
H	Fe38H34C38	HC_2(4);H_2C_2(2);H_6C_9(1);H(1);H_5C_6(1)H_2C(1);H_4C_2(1);H_3C_4 (1);H_5C_4 (1);	H_4C_2 (2);H_2C_2 (9)
I	Fe38H27C34	H_3C_2(1);HC_2(3);H_7C_8(1)C_2 (1);H_3C_4(1);H_2C_2(2);H(1);H_2C_4 (1);H_4C_4 (1)	H_5C_4(1);H_4C_2(2);H_3C_2(2);H_2C_2 (7)
J	Fe38H19C31	H_2C_2(1);C_2(2);HC_2(6);H(2);H_3C_6(1);H_4C_4 (1);H_2C_3(1)	H_4C_2(3);H_6C_3(1);H_2C_2(9);H_5C_2 (1)

Trajectory A: Analysis

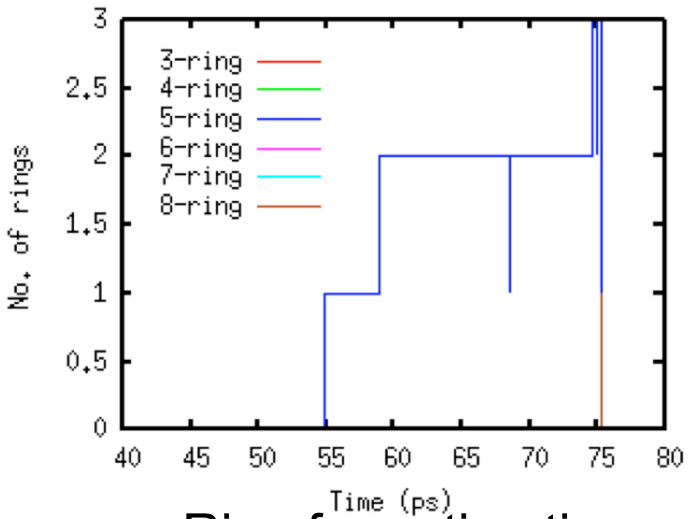

Ring formation time

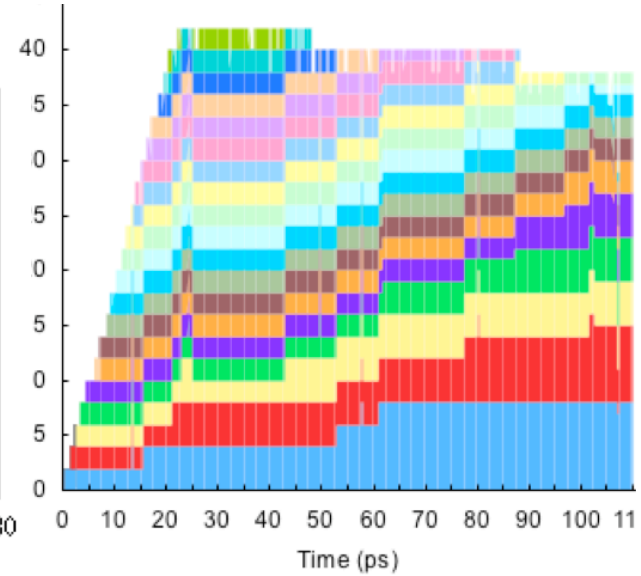

Cluster growth

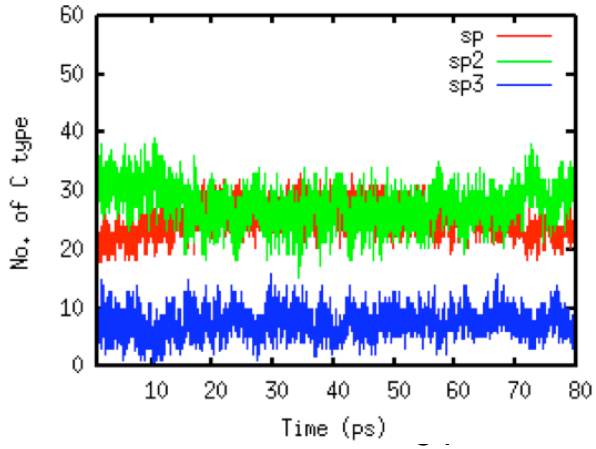

hybridization count

Outline

- Review: Experiments and previous theoretical modeling
- Density-functional tight-binding (DFTB) method
- All-carbon cap nucleation and growth on iron particles
- Comparison of growth mechanisms between iron and nickel catalysts
- Simulation of early stages during ACCVD (C_2H_2 and OH on iron catalyst)
- **Summary and outlook**

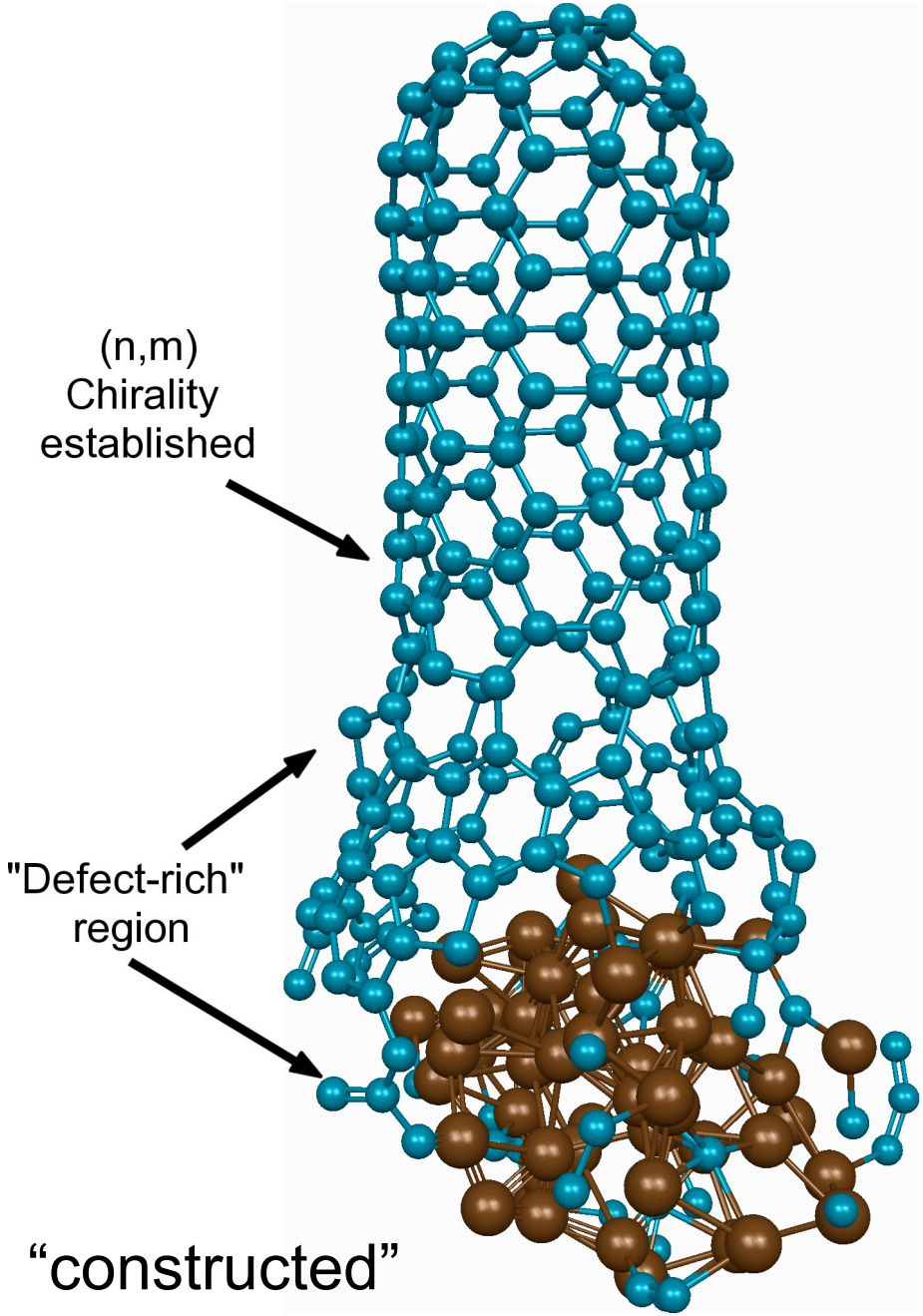

"constructed"

We found:

- **Growth at base is chaotic**
- **Annealing** from pentagon to hexagons **takes place "very slowly"**
- **Weaker C-M adhesion strength allows faster growth (higher C mobility)**

→

(n,m) chirality already established in outer tube area imprints hexagon addition pattern *during annealing*

Summary

- First-ever cap nucleation from bare particle and carbon molecules observed in quantum chemical simulations by slow surface diffusion (**Y-junction and pentagon-first mechanism**)

  - Cap nucleation very **similar to fullerene cage nucleation**, slowed down by presence of metal cluster (immobility of C_2 and polyynes)

- During growth, M/C interface region develops short to longer polyyne chains, picks up carbon and forms 5/6/(7) rings ("arms of the octopus")

  - In continued growth simulations, SWNT (n,m) **chirality NOT preserved!** "Chaotic" growth *caused by rapid carbon supply.*

  - Pentagon-hexagon-only growth achieved by **slower** surface diffusion or addition, **defect annealing** on the order of 10's of ps.

Summary

•Growth on **Ni faster than Fe**, due to lower adhesion energy, Ni less likely to form carbide

- Cap nucleation very **similar to fullerene cage nucleation**, nucleation and growth slowed down by presence of metal cluster (immobility of C_2 and polyynes) *with increasing C-M adhesion*
- diffusion limits growth speed with particle size on simulation time scales

•Acetylene decomposition slow due to **H removal bottleneck**

- H migration slow on carbon, fast on Fe
- H removal mechanism unknown, ideas?
- Role of oxygen is to oxidize, both carbon and iron

Outlook

Present DFTB/MD Simulations

Future Simulations

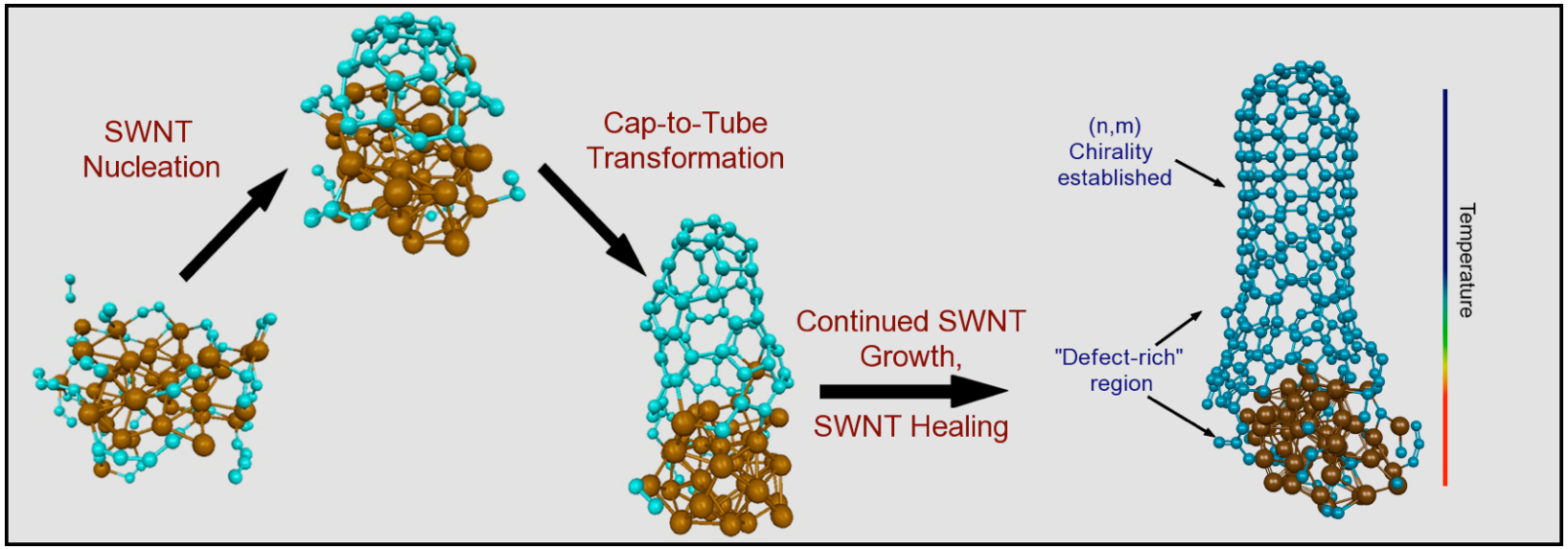

Challenge to Experimentalists:

Can you synthesize edge-oxidized caps of specific type and diameter, attach specific-size metal catalyst, and grow (n,m)-specific tube? *(similar to Smalley's continued growth but with caps instead of tubes)*

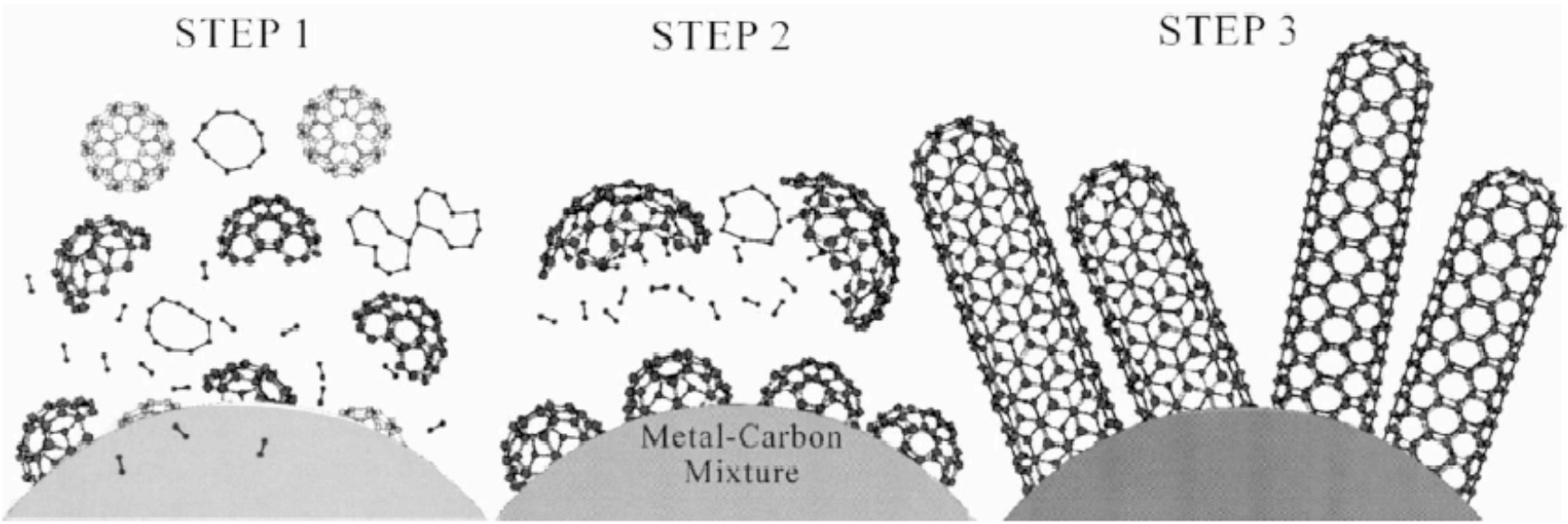

from: Kataura *et al.* Carbon **38**, 1691 (2000)

Note: we do not endorse this mechanism,
Only the picture!

Thank you

Acknowledgements

Funding :

- Japan Science and Technology Agency CREST grant in the Area of High Performance Computing for Multi-scale and Multi-physics Phenomena

- JST Tenure Track Funding by MEXT MSCF (to SI)

Computer resources :

- Research Center for Computational Science (RCCS), Okazaki Research Facilities, National Institutes for Natural Sciences.

- Academic Center for Computing and Media Studies (ACCMS), Kyoto University

Acetylene-Accelerated Alcohol Catalytic Chemical Vapor Deposition Growth of Vertically Aligned Single-Walled Carbon Nanotubes

J. Phys. Chem. C **2009**, *113*, 7511–7515

Rong Xiang,[†] Erik Einarsson,[†] Jun Okawa,[†] Yuhei Miyauchi,[‡] and Shigeo Maruyama*[,†]

Department of Mechanical Engineering, The University of Tokyo, 7-3-1 Hongo, Bunkyo-ku, Tokyo 113-8656, and Institute for Chemical Research, Kyoto University, Uji, Kyoto 611-0011, Japan

Received: November 28, 2008; Revised Manuscript Received: March 12, 2009

Addition of only 1% acetylene into ethanol was found to enhance the growth rate of single-walled carbon nanotubes (SWNTs) by up to 10-fold. This accelerated growth, however, only occurred in the presence of ethanol, whereas pure acetylene at the same partial pressure resulted in negligible growth and quickly deactivated the catalyst. The dormant catalyst could be revived by reintroduction of ethanol, indicating that catalyst deactivation is divided into reversible and irreversible stages. Since the thermal decomposition of ethanol also yields some amount of acetylene, the possible contribution to the formation of SWNTs from these decomposed gases is also discussed.